

3. Wang Q, Curran ME, Splawski I, Burn TC, Millholland JM, Van Raay TJ, Shen J, Timothy KW, Vincent GM, De Jager T, Schwartz PJ, Towbin JA, Moss AJ, Atkinson DL, Landes GM, Connors TD, Keating MT. Positional cloning of a novel potassium channel gene: *KVLQT1* mutations cause cardiac arrhythmias. *Nat Genet.* 1996;12:17–23.
4. Sanguinetti MC, Jiang C, Curran ME, Keating MT. A mechanistic link between an inherited and an acquired cardiac arrhythmia: HERG encodes the  $I_{Kr}$  potassium channel. *Cell.* 1995;81:299–307.
5. Papazian DM, Schwarz TL, Tempel BL, Jan YN, Jan LY. Cloning of genomic and complementary DNA from Shaker, a putative potassium channel gene from *Drosophila*. *Science.* 1987;237:749–753.
6. Zipes DP. The long QT interval syndrome: a Rosetta stone for sympathetic related ventricular tachyarrhythmias. *Circulation.* 1991;84:1414–1419.
7. Nattel S, Yue L, Wang Z. Cardiac ultrarapid delayed rectifiers: a novel potassium current family of functional similarity and molecular diversity. *Cell Physiol Biochem.* 1999;9:217–226.
8. Snyders DJ, Tamkun MM, Bennett PB. A rapidly activating and slowly inactivating potassium channel cloned from human heart: functional analysis after stable mammalian cell culture expression. *J Gen Physiol.* 1999;101:513–543.
9. Hille B. *Ion Channels of Excitable Membranes*. 3rd ed. Sunderland, MA: Sinauer Associates; 2001:131–168.
10. Trudeau MC, Warmke JW, Ganetzky B, Robertson GA. HERG, a human inward rectifier in the voltage-gated potassium channel family. *Science.* 1995;269:92–95.
11. Jiang Y, Lee A, Chen J, Cadene M, Chait BT, MacKinnon R. The open pore conformation of potassium channels. *Nature.* 2002;417:523–526.
12. Seoh SA, Sigg D, Papazian DM, Bezanilla F. Voltage-sensing residues in the S2 and S4 segments of the Shaker  $K^+$  channel. *Neuron.* 1996;16:1159–1167.
13. Ding S, Ingleby L, Ahern CA, Horn R. Investigating the putative glycine hinge in Shaker potassium channel. *J Gen Physiol.* 2005;126:213–226.
14. Pusch M, Magrassi R, Wollnik B, Conti F. Activation and inactivation of homomeric KvLQT1 potassium channels. *Biophys J.* 1998;75:785–792.
15. Sanguinetti MC, Curran ME, Zou A, Shen J, Spector PS, Atkinson DL, Keating MT. Coassembly of KvLQT1 and minK (IsK) proteins to form cardiac  $I_{Ks}$  potassium channel. *Nature.* 1996;384:80–83.
16. Barhanin J, Lesage F, Guillemare E, Fink M, Lazdunski M, Romey G. KvLQT1 and IsK (minK) proteins associate to form the  $I_{Ks}$  cardiac potassium current. *Nature.* 1996;384:78–80.
17. Olson TM, Alekseev AE, Liu XK, Park S, Zingman LV, Bienengraeber M, Sattiraju S, Ballew JD, Jahangir A, Terzic A. Kv1.5 channelopathy due to KCNA5 loss-of-function mutation causes human atrial fibrillation. *Hum Mol Genet.* 2006;15:2185–2191.
18. Yang Y, Li J, Lin X, Yang Y, Hong K, Wang L, Liu J, Li L, Yan D, Liang D, Xiao J, Jin H, Wu J, Zhang Y, Chen YH. Novel KCNA5 loss-of-function mutations responsible for atrial fibrillation. *J Hum Genet.* 2009;54:277–283.
19. Yang T, Yang P, Roden DM, Darbar D. Novel KCNA5 mutation implicates tyrosine kinase signaling in human atrial fibrillation. *Heart Rhythm.* 2010;7:1246–1252.
20. An WF, Bowlby MR, Betty M, Cao J, Ling HP, Mendoza G, Hinson JW, Mattsson KI, Strassle BW, Trimmer JS, Rhodes KJ. Modulation of A-type potassium channels by a family of calcium sensors. *Nature.* 2000;403:553–556.
21. Nakamura TY, Pountney DJ, Ozaita A, Nandi S, Ueda S, Rudy B, Coetzee WA. A role for frequenin, a Ca-binding protein, as a regulator of Kv4 K-currents. *Proc Natl Acad Sci USA.* 2001;98:12808–12813.
22. Radicke S, Cotella D, Graf EM, Banse U, Jost N, Varro A, Tseng GN, Ravens U, Wettwer E. Functional modulation of the transient outward current  $I_{to}$  by KCNE beta-subunits and regional distribution in human non-failing and failing hearts. *Cardiovasc Res.* 2006;71:695–703.
23. Delpon E, Cordeiro JM, Núñez L, Thomsen PEB, Guerschicoff A, Pollevick GD, Wu Y, Kanters JK, Larsen CT, Hofman-Bang J, Burashnikov E, Christiansen M, Antzelevitch C. Functional effects of KCNE3 mutation and its role in the development of Brugada syndrome. *Circ Arrhythm Electrophysiol.* 2008;1:209–218.
24. Wu J, Shimizu W, Ding WG, Ohno S, Toyoda F, Itoh H, Zang WJ, Miyamoto Y, Kamakura S, Matsuura H, Nademanee K, Brugada J, Brugada P, Brugada R, Vatta M, Towbin JA, Antzelevitch C, Horie M. KCNE2 modulation of Kv4.3 current and its potential role in fatal rhythm disorders. *Heart Rhythm.* 2010;7:199–205.
25. Ohno S, Zanko DP, Ding W-G, Makiyama T, Doi T, Shizuta S, Itoh H, Nishio Y, Hattori T, Matsuura H, Horie M. KCNE5 (KCNE1L) variants are novel modulator of Brugada syndrome and idiopathic ventricular fibrillation. *Circ Arrhythm Electrophysiol.* In press.
26. Abbott GW, Sesti F, Splawski I, Buck ME, Lehmann MH, Timothy KW, Keating MT, Goldstein SA. MiRP1 forms  $I_{Kr}$  potassium channels with HERG and is associated with cardiac arrhythmia. *Cell.* 1999;97:175–187.
27. Sesti F, Abbott GW, Wei J, Murray KT, Saksena S, Schwartz PJ, Priori SG, Roden DM, George AL Jr, Goldstein SA. A common polymorphism associated with antibiotic-induced cardiac arrhythmia. *Proc Natl Acad Sci USA.* 2000;97:10613–10618.
28. McDonald TV, Yu Z, Ming Z, Palma E, Meyers MB, Wang KW, Goldstein SA, Fishman GI. A minK-HERG complex regulates the cardiac potassium current  $I_{Kr}$ . *Nature.* 1997;388:289–292.
29. Ohno S, Zankov DP, Yoshida H, Tsuji K, Makiyama T, Itoh H, Akao M, Hancox JC, Kita T, Horie M. N- and C-terminal KCNE1 mutations cause distinct phenotypes of long QT syndrome. *Heart Rhythm.* 2007;4:332–340.
30. Nishio Y, Makiyama T, Itoh H, Sakaguchi T, Ohno S, Gong YZ, Yamamoto S, Ozawa T, Ding WG, Toyoda F, Kawamura M, Akao M, Matsuura H, Kimura T, Kita T, Horie M. D85N, a KCNE1 polymorphism, is a disease-causing gene variant in long QT syndrome. *J Am Coll Cardiol.* 2009;54:812–819.
31. Kubo Y, Baldwin TJ, Jan YN, Jan LY. Primary structure and functional expression of a mouse inward rectifier potassium channel. *Nature.* 1993;362:127–133.
32. Raab-Graham KF, Radeke CM, Vandenberg CA. Molecular cloning and expression of a human heart inward rectifier potassium channel. *Neuroreport.* 1994;5:2501–2105.
33. He C, Yan X, Zhang H, Mirshahi T, Jin T, Huang A, Logothetis DE. Identification of critical residues controlling G protein-gated inwardly rectifying  $K^+$  channel activity through interactions with the beta-gamma subunits of G proteins. *J Biol Chem.* 2002;277:6088–6096.
34. Noma A. ATP-regulated  $K^+$  channels in cardiac muscle. *Nature.* 1983;305:147–148.
35. Inagaki N, Inazawa J, Seino S. cDNA sequence, gene structure, and chromosomal localization of the human ATP-sensitive potassium channel, uKATP-1, gene (KCNJ8). *Genomics.* 1995;30:102–104.
36. Inagaki N, Gonoi T, Clement JP IV, Namba N, Inazawa J, Gonzalez G, Aguilar-Bryan L, Seino S, Bryan J. Reconstitution of IKATP: an inward rectifier subunit plus the sulfonylurea receptor. *Science.* 1995;270:1166–1170.
37. Vandenberg CA. Inward rectification of a potassium channel in cardiac ventricular cells depends on internal magnesium ions. *Proc Natl Acad Sci USA.* 1987;84:2560–2564.
38. Horie M, Irisawa H, Noma A. Voltage-dependent magnesium block of adenosine-triphosphate-sensitive potassium channel in guinea-pig ventricular cells. *J Physiol.* 1987;387:251–272.
39. Lopatin AN, Makhina EN, Nichols CG. Potassium channel block by cytoplasmic polyamines as the mechanism of intrinsic rectification. *Nature.* 1994;372:366–369.
40. Ficker E, Taglialatela M, Wible BA, Henley CM, Brown AM. Spermine and spermidine as gating molecules for inward rectifier  $K^+$  channels. *Science.* 1994;266:1068–1072.
41. Jan LY, Jan YN. Voltage-gated and inwardly rectifying potassium channels. *J Physiol.* 1997;505:267–282.
42. Schwartz PJ, Moss AJ, Vincent GM, Crampton RS. Diagnostic criteria for the long QT syndrome: an update. *Circulation.* 1993;88:782–784.
43. Shimizu W. The long QT syndrome: therapeutic implications of a genetic diagnosis. *Cardiovasc Res.* 2005;67:347–356.
44. Wang Q, Shen J, Splawski I, Atkinson D, Li Z, Robinson JL, Moss AJ, Towbin JA, Keating MT. SCN5A mutations associated with an inherited cardiac arrhythmia, long QT syndrome. *Cell.* 1995;80:805–811.
45. Splawski I, Shen J, Timothy KW, Lehmann MH, Priori S, Robinson JL, Moss AJ, Schwartz PJ, Towbin JA, Vincent GM, Keating MT. Spectrum of mutations in long-QT syndrome genes: KVLQT1, HERG, SCN5A, KCNE1, and KCNE2. *Circulation.* 2000;102:1178–1185.
46. Plaster NM, Tawil R, Tristani-Firouzi M, Cantún S, Bendahhou S, Tsunoda A, Donaldson MR, Iannaccone ST, Brunt E, Barohn R, Clark J, Deymeier F, George AL Jr, Fish FA, Hahn A, Nitu A, Ozdemir C, Serdaroglu P, Subramony SH, Wolfe G, Fu YH, Ptáček LJ. Mutations in *Kir2.1* cause the developmental and episodic electrical phenotypes of Andersen's syndrome. *Cell.* 2001;105:511–519.

47. Mohler PJ, Schott JJ, Gramolini AO, Dilly KW, Guatimosim S, duBell WH, Song LS, Haurogné K, Kyndt F, Ali ME, Rogers TB, Lederer WJ, Escande D, Le Marec H, Bennett V. Ankyrin-B mutation causes type 4 long-QT cardiac arrhythmia and sudden cardiac death. *Nature*. 2003; 421:634–639.
48. Splawski I, Timothy KW, Sharpe LM, Decher N, Kumar P, Bloise R, Napolitano C, Schwartz PJ, Joseph RM, Condouris K, Tager-Flusberg H, Priori SG, Sanguinetti MC, Keating MT. Ca(V)<sub>1.2</sub> calcium channel dysfunction causes a multisystem disorder including arrhythmia and autism. *Cell*. 2004;119:19–31.
49. Vatta M, Ackerman MJ, Ye B, Makielski JC, Ughanze EE, Taylor EW, Tester DJ, Balijepalli RC, Foell JD, Li Z, Kamp TJ, Towbin JA. Mutant caveolin-3 induces persistent late sodium current and is associated with long-QT syndrome. *Circulation*. 2006;114:2104–2112.
50. Medeiros-Domingo A, Kaku T, Tester DJ, Iturralde-Torres P, Ity A, Ye B, Valdivia C, Ueda K, Canizales-Quintero S, Tusie-Luna MT, Makielski JC, Ackerman MJ. SCN4B-encoded sodium channel beta4 subunit in congenital long-QT syndrome. *Circulation*. 2007;116:134–142.
51. Chen L, Marquardt ML, Tester DJ, Sampson KJ, Ackerman MJ, Kass RS. Mutation of an A-kinase-anchoring protein causes long-QT syndrome. *Proc Natl Acad Sci USA*. 2007;104:20990–20995.
52. Ueda K, Valdivia C, Medeiros-Domingo A, Tester DJ, Vatta M, Farrugia G, Ackerman MJ, Makielski JC. Syntrophin mutation associated with long QT syndrome through activation of the nNOS-SCN5A macromolecular complex. *Proc Natl Acad Sci USA*. 2008;105:9355–9360.
53. Wu G, Ai T, Kim JJ, Mohapatra B, Xi Y, Li Z, Abbasi S, Purevjav E, Samani K, Ackerman MJ, Qi M, Moss AJ, Shimizu W, Towbin JA, Cheng J, Vatta M. Alpha-1-syntrophin mutation and the long QT syndrome: a disease of sodium channel disruption. *Circ Arrhythm Electrophysiol*. 2008;1:193–201.
54. Yang Y, Yang Y, Liang B, Liu J, Li J, Grunnet M, Olesen SP, Rasmussen HB, Ellinor PT, Gao L, Lin X, Li L, Wang L, Xiao J, Liu Y, Liu Y, Zhang S, Liang D, Peng L, Jespersen T, Chen YH. Identification of a Kir3.4 mutation in congenital long QT syndrome. *Am J Hum Genet*. 2010;86:872–880.
55. Ai T, Fujiwara Y, Tsuji K, Otani H, Nakano S, Kubo Y, Horie M. Novel KCNJ2 mutation in familial periodic paralysis with ventricular dysrhythmia. *Circulation*. 2002;105:2592–2594.
56. Vega A, Tester D, Ackerman M, Makielski J. Protein kinase A-dependent biophysical phenotype for V227F-KCNJ2 mutation in catecholaminergic polymorphic ventricular tachycardia. *Circ Arrhythm Electrophysiol*. 2009;2:540–577.
57. Splawski I, Timothy KW, Vincent GM, Atkinson DL, Keating MT. Molecular basis of the long-QT syndrome associated with deafness. *N Engl J Med*. 1997;336:1562–1567.
58. Schwartz PJ, Crotti L. Can a message from the dead save lives? *J Am Coll Cardiol*. 2007;49:247–249.
59. Rhodes TE, Abraham RL, Welch RC, Vanoye CG, Crotti L, Arnestad M, Insolia R, Pedrazzini M, Ferrandi C, Vege A, Rognum T, Roden DM, Schwartz PJ, George AL Jr. Cardiac potassium channel dysfunction in sudden infant death syndrome. *J Mol Cell Cardiol*. 2008;44:571–581.
60. Moss AJ, Zareba W, Benhorin J, Locati EH, Hall WJ, Robinson JL, Schwartz PJ, Towbin JA, Vincent GM, Lehmann MH. ECG T-wave patterns in genetically distinct forms of the hereditary long QT syndrome. *Circulation*. 1995;92:2929–2934.
61. Takenaka K, Ai T, Shimizu W, Kobori A, Ninomiya T, Otani H, Kubota T, Takaki H, Kamakura S, Horie M. Exercise stress test amplifies genotype-phenotype correlation in the LQT1 and LQT2 forms of the long QT syndrome. *Circulation*. 2003;107:838–844.
62. Shimizu W, Antzelevitch C. Sodium channel block with mexiletine is effective in reducing dispersion of repolarization and preventing torsade de pointes in LQT2 and LQT3 models of the long-QT syndrome. *Circulation*. 1997;96:2038–2047.
63. Shimizu W, Antzelevitch C. Cellular basis for the electrocardiographic features of the LQT1 form of the long QT syndrome: effects of  $\beta$ -adrenergic agonists, antagonists and sodium channel blockers on transmural dispersion of repolarization and torsade de pointes. *Circulation*. 1998;98:2314–2322.
64. Shimizu W, Antzelevitch C. Differential effects of beta-adrenergic agonists and antagonists in LQT1, LQT2 and LQT3 models of the long QT syndrome. *J Am Coll Cardiol*. 2000;35:778–86.
65. Morita H, Zipes DP, Morita ST, Wu J. Mechanism of U wave and polymorphic ventricular tachycardia in a canine tissue model of Andersen-Tawil syndrome. *Cardiovasc Res*. 2007;75:510–518.
66. Zareba W, Moss AJ, Schwartz PJ, Vincent GM, Robinson JL, Priori SG, Benhorin J, Locati EH, Towbin JA, Keating MT, Lehmann MH, Hall WJ. Influence of the genotype on the clinical course of the long-QT syndrome. *N Engl J Med*. 1998;339:960–965.
67. Priori SG, Schwartz PJ, Napolitano C, Bloise R, Ronchetti E, Grillo M, Vicentini A, Spazzolini C, Nastoli J, Bottelli G, Folli R, Cappelletti D. Risk stratification in the long-QT syndrome. *N Engl J Med*. 2003;348:1866–1874.
68. Wang D, Crotti L, Shimizu W, Pedrazzini M, Cantu F, De Filippo P, Kishiki K, Miyazaki A, Ikeda T, Schwartz PJ, George AL. Malignant perinatal variant of long-QT syndrome caused by a profoundly dysfunctional cardiac sodium channel mutation. *Circ Arrhythm Electrophysiol*. 2008;1:370–378.
69. Locati EH, Zareba W, Moss AJ, Schwartz PJ, Vincent GM, Lehmann MH, Towbin JA, Priori SG, Napolitano C, Robinson JL, Andrews M, Timothy K, Hall WJ. Age- and sex-related differences in clinical manifestations in patients with congenital long-QT syndrome: findings from the international LQTS registry. *Circulation*. 1998;97:2237–2244.
70. Moss AJ, Shimizu W, Wilde AAM, Towbin JA, Zareba Z, Robinson JL, Qi M, Vincent GM, Ackerman MJ, Kaufman ES, Hofman N, Seth R, Kamakura S, Miyamoto Y, Goldenberg I, Andrews ML, McNitt S. Clinical aspects of type-1 long-QT syndrome by location, coding type, and biophysical function of mutations involving the KCNQ1 gene. *Circulation*. 2007;115:2481–2489.
71. Shimizu W, Moss AJ, Wilde AAM, Towbin JA, Ackerman MJ, January C, Tester DJ, Zareba W, Robinson JL, Qi M, Vincent GM, Kaufman ES, Hofman N, Noda T, Kamakura S, Miyamoto Y, MD, Shah S, Amin V, Goldenberg I, Andrews ML, McNitt S. Genotype-phenotype aspects of type-2 long-QT syndrome. *J Am Coll Cardiol*. 2009;54:2052–2062.
72. Schwartz PJ, Priori SG, Spazzolini C, Moss AJ, Vincent GM, Napolitano C, Denjoy I, Guicheney P, Breithardt G, Keating MT, Towbin JA, Beggs AH, Brink P, Wilde AA, Toivonen L, Zareba W, Robinson JL, Timothy KW, Corfield V, Wattanasirichaigoon D, Corbett C, Haverkamp W, Schulze-Bahr E, Lehmann MH, Schwartz K, Coumel P, Bloise R. Genotype-phenotype correlation in the long-QT syndrome: gene-specific triggers for life-threatening arrhythmias. *Circulation*. 2001;103:89–95.
73. Wilde AAM, Jongbloed RJE, Doevendans PA, Duren DR, Hauer RNW, van Langen IM, van Tintelen JP, Smeets HJ, Meyer H, Geelen JL. Auditory stimuli as a trigger for arrhythmic events differentiate HERG-related (LQT2) patients from KVLQT1-related patients (LQT1). *J Am Coll Cardiol*. 1999;33:327–332.
74. Khositseth A, Tester DJ, Will ML, Bell CM, Ackerman MJ. Identification of a common genetic substrate underlying postpartum cardiac events in congenital long QT syndrome. *Heart Rhythm*. 2004;1:60–64.
75. Shimizu W, Noda T, Takaki H, Kurita T, Nagaya N, Satomi K, Suyama K, Aihara N, Kamakura S, Sunagawa K, Echigo S, Nakamura K, Ohe T, Towbin JA, Napolitano C, Priori SG. Epinephrine unmasks latent mutation carriers with LQT1 form of congenital long QT syndrome. *J Am Coll Cardiol*. 2003;41:633–642.
76. Shimizu W, Noda T, Takaki H, Nagaya N, Satomi K, Kurita T, Suyama K, Aihara N, Sunagawa K, Echigo S, Miyamoto Y, Yoshimasa Y, Nakamura K, Ohe T, Towbin JA, Priori SG, Kamakura S. Diagnostic value of epinephrine test for genotyping LQT1, LQT2 and LQT3 forms of congenital long QT syndrome. *Heart Rhythm*. 2004;1:276–283.
77. Vyas H, Hejlik J, Ackerman MJ. Epinephrine QT stress testing in the evaluation of congenital long-QT syndrome: diagnostic accuracy of the paradoxical QT response. *Circulation*. 2006;113:1385–1392.
78. Shimizu W, Ackerman MJ. Provocative testing in inherited arrhythmias. In: Gussak I, Antzelevitch C, Wilde A, Friedman P, Ackerman MJ, Shen WK, eds. *Electrical Diseases of the Heart: Genetics, Mechanisms, Treatment, Prevention*. London, United Kingdom: Springer; 2007: 424–433.
79. Goldenberg I, Horr S, Moss AJ, Lopes CM, Barsheshet A, McNitt S, Zareba W, Andrews ML, Robinson JL, Locati EH, Ackerman MJ, Benhorin J, Kaufman ES, Napolitano C, Platonov PG, Priori SG, Qi M, Schwartz PJ, Shimizu W, Towbin JA, Vincent GM, Wilde AA, Zhang L. Risk for life-threatening cardiac events in patients with genotype-confirmed long-QT syndrome and normal-range corrected QT intervals. *J Am Coll Cardiol*. 2010;57:51–59.
80. Viskin S, Postema PG, Bhuiyan ZA, Rosso R, Kalman JM, Vohra JK, Guevara-Valdivia ME, Marquez MF, Kogan E, Belhassen B, Glikson M, Strasberg B, Antzelevitch C, Wilde AA. The response of the QT interval to the brief tachycardia provoked by standing: a bedside test for diagnosing long QT syndrome. *J Am Coll Cardiol*. 2010;55:1955–1961.

81. Shimizu W. Clinical impact of genetic studies in lethal inherited cardiac arrhythmias. *Circ J*. 2008;72:1926–1936.
82. Vincent GM, Schwartz PJ, Denjoy I, Swan H, Bithell C, Spazzolini C, Crotti L, Piippo K, Lupoglazoff JM, Villain E, Priori SG, Napolitano C, Zhang L. High efficacy of beta-blockers in long-QT syndrome type 1: contribution of noncompliance and QT-prolonging drugs to the occurrence of beta-blocker treatment "failures." *Circulation*. 2009;119:215–221.
83. Schwartz PJ. Cutting nerves and saving lives. *Heart Rhythm*. 2009;6:760–763.
84. Priori SG, Napolitano C, Schwartz PJ, Grillo M, Bloise R, Ronchetti E, Moncalvo C, Tulipani C, Veia A, Bottelli G, Nastoli J. Association of long QT syndrome loci and cardiac events among patients treated with beta-blockers. *JAMA*. 2004;292:1341–1344.
85. Compton SJ, Lux RL, Ramsey MR, Strellich KR, Sanguinetti MC, Green LS, Keating MT, Mason JW. Genetically defined therapy of inherited long-QT syndrome: correction of abnormal repolarization by potassium. *Circulation*. 1996;94:1018–1022.
86. Noda T, Takaki H, Kurita T, Suyama K, Nagaya N, Taguchi A, Aihara N, Kamakura S, Sunagawa K, Nakamura K, Ohe T, Horie M, Napolitano C, Towbin JA, Priori SG, Shimizu W. Gene-specific response of dynamic ventricular repolarization to sympathetic stimulation in LQT1, LQT2 and LQT3 forms of congenital long QT syndrome. *Eur Heart J*. 2002;23:975–983.
87. Tan HL, Bardia A, Shimizu W, Moss AJ, Schulze-Bahr E, Noda T, Wilde AA. Genotype-specific onset of arrhythmias in congenital long QT syndrome: possible therapy implications. *Circulation*. 2006;114:2096–2103.
88. Shimizu W, Horie M, Ohno S, Takenaka K, Yamaguchi M, Shimizu M, Washizuka T, Aizawa Y, Nakamura K, Ohe T, Aiba T, Miyamoto Y, Yoshimasa Y, Towbin JA, Priori SG, Kamakura S. Mutation site-specific differences in arrhythmic risk and sensitivity to sympathetic stimulation in LQT1 form of congenital long QT syndrome: multicenter study in Japan. *J Am Coll Cardiol*. 2004;44:117–125.
89. Moss AJ, Zareba W, Kaufman ES, Gartman E, Peterson DR, Benhorin J, Towbin JA, Keating MT, Priori SG, Schwartz PJ, Vincent GM, Robinson JL, Andrews ML, Feng C, Hall WJ, Medina A, Zhang L, Wang Z. Increased risk of arrhythmic events in long-QT syndrome with mutations in the pore region of the human ether-a-go-go-related gene potassium channel. *Circulation*. 2002;105:794–799.
90. Gussak I, Brugada P, Brugada J, Wright RS, Kopecky SL, Chaitman BR, Bjerregaard P. Idiopathic short QT interval: a new clinical syndrome? *Cardiology*. 2000;94:99–102.
91. Gaita F, Giustetto C, Bianchi F, Wolpert C, Schimpf R, Riccardi R, Grossi S, Richiardi E, Borggrefe M. Short QT syndrome: a familial cause of sudden death. *Circulation*. 2003;108:965–970.
92. Lehnart SE, Ackerman MJ, Benson DW Jr, Brugada R, Clancy CE, Donahue JK, George AL Jr, Grant AO, Groft SC, January CT, Lathrop DA, Lederer WJ, Makielski JC, Mohler PJ, Moss A, Nerbonne JM, Olson TM, Przywara DA, Towbin JA, Wang LH, Marks AR. Inherited arrhythmias: a National Heart, Lung, and Blood Institute and Office of Rare Diseases workshop consensus report about the diagnosis, phenotyping, molecular mechanisms, and therapeutic approaches for primary cardiomyopathies of gene mutations affecting ion channel function. *Circulation*. 2007;116:2325–2345.
93. Viskin S. The QT interval: too long, too short or just right. *Heart Rhythm*. 2009;6:711–715.
94. Brugada R, Hong K, Dumaine R, Cordeiro J, Gaita F, Borggrefe M, Menendez TM, Brugada J, Pollevick GD, Wolpert C, Burashnikov E, Matsuo K, Wu YS, Guerschicoff A, Bianchi F, Giustetto C, Schimpf R, Brugada P, Antzelevitch C. Sudden death associated with short-QT syndrome linked to mutations in HERG. *Circulation*. 2004;109:30–35.
95. Belloq C, van Ginneken AC, Bezzina CR, Alders M, Escande D, Mannens MM, Baró I, Wilde AA. Mutation in the KCNQ1 gene leading to the short QT-interval syndrome. *Circulation*. 2004;109:2394–2397.
96. Priori SG, Pandit SV, Rivolta I, Berenfeld O, Ronchetti E, Dharmoon A, Napolitano C, Anumonwo J, di Barletta MR, Gudapakkam S, Bosi G, Stramba-Badiale M, Jalife J. A novel form of short QT syndrome (SQT3) is caused by a mutation in the KCNJ2 gene. *Circ Res*. 2005;96:800–807.
97. Extramiana F, Antzelevitch C. Amplified transmural dispersion of repolarization as the basis for arrhythmogenesis in a canine ventricular-wedge model of short-QT syndrome. *Circulation*. 2004;110:3661–3666.
98. Watanabe H, Makiyama T, Koyama T, Kannankeril PJ, Seto S, Okamura K, Oda H, Ito H, Okada M, K, Tanabe N, Kamakura K, Horie M, Aizawa Y, Shimizu W. High prevalence of early repolarization in short QT syndrome. *Heart Rhythm*. 2010;7:647–652.
99. Gaita F, Giustetto C, Bianchi F, Schimpf R, Haissaguerre M, Calò L, Brugada R, Antzelevitch C, Borggrefe M, Wolpert C. Short QT syndrome: pharmacological treatment. *J Am Coll Cardiol*. 2004;43:1494–1499.
100. Brugada P, Brugada J. Right bundle branch block, persistent ST segment elevation and sudden cardiac death: a distinct clinical and electrocardiographic syndrome: a multicenter report. *J Am Coll Cardiol*. 1992;20:1391–1396.
101. Priori SG, Napolitano C, Gasparini M, Pappone C, Della Bella P, Giordano U, Bloise R, Giustetto C, De Nardis R, Grillo M, Ronchetti E, Faggiano G, Nastoli J. Natural history of Brugada syndrome: insights for risk stratification and management. *Circulation*. 2002;105:1342–1347.
102. Antzelevitch C, Brugada P, Borggrefe M, Brugada J, Brugada R, Corrado D, Gussak I, LeMarec H, Nademanee K, Perez Riera AR, Shimizu W, Schulze-Bahr E, Tan H, Wilde A. Brugada syndrome: report of the Second Consensus Conference: endorsed by the Heart Rhythm Society and the European Heart Rhythm Association. *Circulation*. 2005;111:659–670.
103. Shimizu W, Aiba T, Kamakura S. Mechanisms of disease: current understanding and future challenges in Brugada syndrome. *Nat Clin Pract Cardiovasc Med*. 2005;2:408–414.
104. Chen Q, Kirsch GE, Zhang D, Brugada R, Brugada J, Brugada P, Potenza D, Moya A, Borggrefe M, Breithardt G, Ortiz-Lopez R, Wang Z, Antzelevitch C, O'Brien RE, Schulze-Bahr E, Keating MT, Towbin JA, Wang Q. Genetic basis and molecular mechanisms for idiopathic ventricular fibrillation. *Nature*. 1998;392:293–296.
105. Kapplinger JD, Tester DJ, Alders M, Benito B, Berthet M, Brugada J, Brugada P, Fressart V, Guerschicoff A, Harris-Kerr C, Kamakura S, Kyndt F, Koopmann TT, Miyamoto Y, Pfeiffer R, Pollevick GD, Probst V, Zumhagen S, Vatta M, Towbin JA, Shimizu W, Schulze-Bahr E, Antzelevitch C, Salisbury BA, Guicheney P, Wilde AA, Brugada R, Schott JJ, Ackerman MJ. An international compendium of mutations in the SCN5A-encoded cardiac sodium channel in patients referred for Brugada syndrome genetic testing. *Heart Rhythm*. 2010;7:33–46.
106. Shimizu W. Acquired form of Brugada syndrome. In: Gussak I, Antzelevitch C, Wilde A, Friedman P, Ackerman MJ, Shen WK, eds. *Electrical Diseases of the Heart: Genetics, Mechanisms, Treatment, Prevention*. London, United Kingdom: Springer; 2007:719–728.
107. Gussak I, Antzelevitch C. Early repolarization syndrome: clinical characteristics and possible cellular and ionic mechanisms. *J Electrocardiol*. 2000;33:299–309.
108. Haissaguerre M, Derval N, Sacher F, Jesel L, Deisenhofer I, de Roy L, Pasquie JL, Nogami A, Babuty D, Yi-Mayry S, De Chillou C, Scanu P, Mabo P, Matsuo S, Probst V, Le Scouarnec S, Defaye P, Schlaepfer J, Rostock T, Lacroix D, Lamaison D, Lavergne T, Aizawa Y, Englund A, Anselme F, O'Neill M, Hocini M, Lim KT, Knecht S, Veenhuizen GD, Bordachar P, Chauvin M, Jais P, Coureau G, Chene G, Klein GJ, Clémenty J. Sudden cardiac arrest associated with early repolarization. *N Engl J Med*. 2008;358:2016–2023.
109. Haissaguerre M, Chatel S, Sacher F, Weerasooriya R, Probst V, Lous-souarn G, Horlitz M, Liersch R, Schulze-Bahr E, Wilde A, Käab S, Koster J, Rudy Y, Le Marec H, Schott JJ. Ventricular fibrillation with prominent early repolarization associated with a rare variant of KCNJ8/KATP channel. *J Cardiovasc Electrophysiol*. 2009;20:93–98.
110. Medeiros-Domingo A, Tan BH, Crotti L, Tester DJ, Eckhardt L, Cuoretti A, Kroboth SL, Song C, Zhou Q, Kopp D, Schwartz PJ, Makielski JC, Ackerman MJ. Gain-of-function mutation S422L in the KCNJ8-encoded cardiac KATP channel Kir6.1 as a pathogenic substrate for J-wave syndromes. *Heart Rhythm*. 2010;7:1466–1471.
111. Fox CS, Parise H, D'Agostino RB Sr, Lloyd-Jones DM, Vasan RS, Wang TJ, Levy D, Wolf PA, Benjamin EJ. Parental atrial fibrillation as a risk factor for atrial fibrillation in offspring. *JAMA*. 2004;291:2851–2855.
112. Chen YH, Xu SJ, Bendahhou S, Wang XL, Wang Y, Xu WY, Jin HW, Sun H, Su XY, Zhuang QN, Yang YQ, Li YB, Liu Y, Xu HJ, Li XF, Ma N, Mou CP, Chen Z, Barhanin J, Huang W. KCNQ1 gain-of-function mutation in familial atrial fibrillation. *Science*. 2003;299:251–254.
113. Yang Y, Xia M, Jin Q, Bendahhou S, Shi J, Chen Y, Liang B, Lin J, Liu Y, Liu B, Zhou Q, Zhang D, Wang R, Ma N, Su X, Niu K, Pei Y, Xu W, Chen Z, Wan H, Cui J, Barhanin J, Chen Y. Identification of a

- KCNE2 gain-of-function mutation in patients with familial atrial fibrillation. *Am J Hum Genet.* 2004;75:899–905.
114. Zhang DF, Liang B, Lin J, Liu B, Zhou QS, Yang YQ. KCNE3 R53H substitution in familial atrial fibrillation. *Chin Med J (Engl).* 2005;118:1735–1738.
  115. Xia M, Jin Q, Bendahhou S, He Y, Larroque MM, Chen Y, Zhou Q, Yang Y, Liu Y, Liu B, Zhu Q, Zhou Y, Lin J, Liang B, Li L, Dong X, Pan Z, Wang R, Wan H, Qiu W, Xu W, Eurlings P, Barhanin J, Chen Y. A Kir2.1 gain-of-function mutation underlies familial atrial fibrillation. *Biochem Biophys Res Commun.* 2005;332:1012–1019.
  116. Burashnikov A, Antzelevitch C. Can inhibition of  $I_{Kur}$  promote atrial fibrillation? *Heart Rhythm.* 2008;5:1304–1309.
  117. Hong K, Bjerregaard P, Gussak I, Brugada R. Short QT syndrome and atrial fibrillation caused by mutation in KCNH2. *J Cardiovasc Electro-physiol.* 2005;16:394–396.
  118. Abraham RL, Yang T, Blair M, Roden DM, Darbar D. Augmented potassium current is a shared phenotype for two genetic defects associated with familial atrial fibrillation. *J Mol Cell Cardiol.* 2010;48:181–190.
  119. Murray A, Donger C, Fenske C, Spillman I, Richard P, Dong YB, Neyroud N, Chevalier P, Denjoy I, Carter N, Syrris P, Afzal AR, Patton MA, Guicheney P, Jeffery S. Splicing mutations in KCNQ1: a mutation hot spot at codon 344 that produces in frame transcripts. *Circulation.* 1999;100:1077–1084.
  120. Tsuji K, Akao M, Ishii TM, Ohno S, Makiyama T, Takenaka K, Doi T, Haruna Y, Yoshida H, Nakashima T, Kita T, Horie M. Mechanistic basis for the pathogenesis of long QT syndrome associated with a common splicing mutation in KCNQ1 gene. *J Mol Cell Cardiol.* 2007;42:662–669.
  121. Gong Q, Zhang L, Vincent GM, Horne BD, Zhou Z. Nonsense mutations in hERG cause a decrease in mutant mRNA transcripts by nonsense-mediated mRNA decay in human long-QT syndrome. *Circulation.* 2007;116:17–24.
  122. Bhuiyan ZA, Momenah TS, Gong Q, Amin AS, Ghamdi SA, Carvalho JS, Homfray T, Mannens MM, Zhou Z, Wilde AA. Recurrent intra-uterine fetal loss due to near absence of HERG: clinical and functional characterization of a homozygous nonsense HERG Q1070X mutation. *Heart Rhythm.* 2008;5:553–561.
  123. Paulussen AD, Gilissen RA, Armstrong M, Doevendans PA, Verhasselt P, Smeets HJ, Schulze-Bahr E, Haverkamp W, Breithardt G, Cohen N, Aerssens J. Genetic variations of KCNQ1, KCNH2, SCN5A, KCNE1, and KCNE2 in drug-induced long QT syndrome patients. *J Mol Med.* 2004;82:182–188.
  124. Bisgaard AM, Rackauskaite G, Thelle T, Kirchoff M, Bryndorf T. Twins with mental retardation and an interstitial deletion 7q34q36.2 leading to the diagnosis of long QT syndrome. *Am J Med Genet A.* 2006;140:644–648.
  125. Koopmann TT, Alders M, Jongbloed RJ, Guerrero S, Mannens MM, Wilde AA, Bezzina CR. Long QT syndrome caused by a large duplication in the KCNH2 (HERG) gene undetectable by current polymerase chain reaction-based exon-scanning methodologies. *Heart Rhythm.* 2006;3:52–55.
  126. Eddy CA, MacCormick JM, Chung SK, Crawford JR, Love DR, Rees MI, Skinner JR, Shelling AN. Identification of large gene deletions and duplications in KCNQ1 and KCNH2 in patients with long QT syndrome. *Heart Rhythm.* 2008;5:1275–1281.
  127. Barc J, Bricc F, Schmitt S, Kyndt F, Le Cunff M, Baron E, Vieyres C, Sacher F, Redon R, Le Caignec C, Le Marec H, Probst V, Schott JJ. Screening for copy number variation in genes associated with the long QT syndrome: clinical relevance. *J Am Coll Cardiol.* 2011;57:40–47.
  128. Yamashita F, Horie M, Kubota T, Yoshida H, Yumoto Y, Kobori A, Ninomiya T, Kono Y, Haruna T, Tsuji K, Washizuka T, Takano M, Otani H, Sasayama S, Aizawa Y. Characterization and subcellular localization of KCNQ1 with a heterozygous mutation in the C terminus. *J Mol Cell Cardiol.* 2001;33:197–207.
  129. Gouas L, Bellocq C, Berthet M, Potet F, Demolombe S, Forhan A, Lescasse R, Simon F, Balkau B, Denjoy I, Hainque B, Baro I, Guicheney P; D.E.S.I.R. Study Group. New KCNQ1 mutations leading to haploinsufficiency in a general population: defective trafficking of a KvLQT1 mutant. *Cardiovasc Res.* 2004;63:60–68.
  130. Aizawa Y, Ueda K, Wu LM, Inagaki N, Hayashi T, Takahashi M, Ohta M, Kawano S, Hirano Y, Yasunami M, Aizawa Y, Kimura A, Hiraoka M. Truncated KCNQ1 mutant, A178fs/105, forms hetero-multimer channel with wild-type causing a dominant-negative suppression due to trafficking defect. *FEBS Lett.* 2004;574:145–150.
  131. Anderson CL, Delisle BP, Anson BD, Kilby JA, Will ML, Tester DJ, Gong Q, Zhou Z, Ackerman MJ, January CT. Most LQT2 mutations reduce Kv11.1 (hERG) current by a class 2 (trafficking-deficient) mechanism. *Circulation.* 2006;113:365–373.
  132. Amin AS, Herfst LJ, Delisle BP, Klemens CA, Rook MB, Bezzina CR, Underkofler HA, Holzem KM, Ruijter JM, Tan HL, January CT, Wilde AA. Fever-induced QTc prolongation and ventricular arrhythmias in individuals with type 2 congenital long QT syndrome. *J Clin Invest.* 2008;118:2552–2561.
  133. Ma D, Zerangue N, Lin YF, Collins A, Yu M, Jan YN, Jan LY. Role of ER export signals in controlling surface potassium channel numbers. *Science.* 2001;291:316–319.
  134. Doi T, Makiyama T, Haruna Y, Tsuji K, Ohno S, Kato M, Akao M, Takahashi Y, Kimura T, Horie M. A novel KCNJ2 nonsense mutation, S369X, impedes trafficking and causes a limited form of Andersen-Tawil syndrome. *Circ Cardiovasc Genet.* In press.
  135. Ehrlich JR, Pourrier M, Weerapura M, Ethier N, Marmabachi AM, Hébert TE, Nattel S. KvLQT1 modulates the distribution and biophysical properties of HERG: a novel alpha-subunit interaction between delayed rectifier currents. *J Biol Chem.* 2004;279:1233–1241.
  136. Brunner M, Peng X, Liu GX, Ren XQ, Ziv O, Choi BR, Mathur R, Hajjiri M, Odening KE, Steinberg E, Folco EJ, Pringa E, Centracchio J, Macharzina RR, Donahay T, Schofield L, Rana N, Kirk M, Mitchell GF, Poppas A, Zehender M, Koren C. Mechanisms of cardiac arrhythmias and sudden death in transgenic rabbits with long QT syndrome. *J Clin Invest.* 2008;118:2246–2259.
  137. Biliczki P, Girmatsion Z, Brandes RP, Harenkamp S, Pitard B, Charpentier F, Hébert TE, Hohnloser SH, Baró I, Nattel S, Ehrlich JR. Trafficking-deficient long QT syndrome mutation KCNQ1-T587M confers severe clinical phenotype by impairment of KCNH2 membrane localization: evidence for clinically significant  $I_{Kr}$ - $I_{Ks}$  alpha-subunit interaction. *Heart Rhythm.* 2009;6:1792–1801.
  138. Saucerman JJ, Healy SN, Belik ME, Puglisi JL, McCulloch AD. Proarrhythmic consequences of a KCNQ1 AKAP-binding domain mutation: computational models of whole cells and heterogeneous tissue. *Circ Res.* 2004;95:1216–1224.
  139. Logothetis DE, Petrou VI, Adney SK, Mahajan R. Channelopathies linked to plasma membrane phosphoinositides. *Pflugers Arch.* 2010;460:321–341.
  140. Balse E, El-Haou S, Dillanian G, Dauphin A, Eldstrom J, Fedida D, Coulombe A, Hatem SN. Cholesterol modulates the recruitment of Kv1.5 channels from Rab11-associated recycling endosome in native atrial myocytes. *Proc Natl Acad Sci U S A.* 2009;106:14681–14686.
  141. Kruse M, Schulze-Bahr E, Corfield V, Beckmann A, Stallmeyer B, Kurtbay G, Ohmert I, Schulze-Bahr E, Brink P, Pongs O. Impaired endocytosis of the ion channel TRPM4 is associated with human progressive familial hear block type 1. *J Clin Invest.* 2009;119:2737–2744.
  142. Liu H, El Zein L, Kruse M, Guinamad R, Beckmann A, Bozio A, Kurtbay G, Mégarbané A, Ohmert I, Blaysat G, Villain E, Pongs O, Bouvagnet P. Gain-of-function mutations in TRPM4 cause autosomal dominant isolated cardiac conduction disease. *Circ Cardiovasc Genet.* 2010;3:374–385.
  143. Li P, Ninomiya H, Kurata Y, Kato M, Miale J, Yamamoto Y, Igawa O, Nakai A, Higaki K, Toyoda F, Wu J, Horie M, Matsuura H, Yoshida A, Shirayoshi Y, Hiraoka M, Hisatome I. Reciprocal control of hERG stability by Hsp70 and Hsc70 with implication for restoration of LQT2 mutant stability. *Circ Res.* In press.
  144. Moretti A, Bellin M, Welling A, Jung CB, Lam JT, Bott-Flügel L, Dorn T, Goedel A, Höhnke C, Hofmann F, Seyfarth M, Sinnecker D, Schömig A, Laugwitz KL. Patient-specific induced pluripotent stem-cell models for long-QT syndrome. *N Engl J Med.* 2010;363:1397–1409.

## Striking In Vivo Phenotype of a Disease-Associated Human *SCN5A* Mutation Producing Minimal Changes in Vitro

Hiroshi Watanabe, MD, PhD, FESC; Tao Yang, PhD; Dina Myers Stroud, PhD; John S. Lowe, PhD; Louise Harris, MD; Thomas C. Atack, BS; Dao W. Wang, MD, PhD; Susan B. Hipkens, PhD; Brenda Leake, BS; Lynn Hall, MS; Sabina Kupersmidt, PhD; Nagesh Chopra, MD; Mark A. Magnuson, MD; Naohito Tanabe, MD, PhD; Björn C. Knollmann, MD, PhD; Alfred L. George, Jr, MD; Dan M. Roden, MD

**Background**—The D1275N *SCN5A* mutation has been associated with a range of unusual phenotypes, including conduction disease and dilated cardiomyopathy, as well as atrial and ventricular tachyarrhythmias. However, when D1275N is studied in heterologous expression systems, most studies show near-normal sodium channel function. Thus, the relationship of the variant to the clinical phenotypes remains uncertain.

**Methods and Results**—We identified D1275N in a patient with atrial flutter, atrial standstill, conduction disease, and sinus node dysfunction. There was no major difference in biophysical properties between wild-type and D1275N channels expressed in Chinese hamster ovary cells or tsA201 cells in the absence or presence of  $\beta 1$  subunits. To determine D1275N function in vivo, the *Scn5a* locus was modified to knock out the mouse gene, and the full-length wild-type (H) or D1275N (DN) human *SCN5A* cDNAs were then inserted at the modified locus by recombinase mediated cassette exchange. Mice carrying the DN allele displayed slow conduction, heart block, atrial fibrillation, ventricular tachycardia, and a dilated cardiomyopathy phenotype, with no significant fibrosis or myocyte disarray on histological examination. The DN allele conferred gene-dose-dependent increases in *SCN5A* mRNA abundance but reduced sodium channel protein abundance and peak sodium current amplitudes (H/H,  $41.0 \pm 2.9$  pA/pF at  $-30$  mV; DN/H,  $19.2 \pm 3.1$  pA/pF,  $P < 0.001$  vs H/H; DN/DN,  $9.3 \pm 1.1$  pA/pF,  $P < 0.001$  versus H/H).

**Conclusions**—Although D1275N produces near-normal currents in multiple heterologous expression experiments, our data establish this variant as a pathological mutation that generates conduction slowing, arrhythmias, and a dilated cardiomyopathy phenotype by reducing cardiac sodium current. (*Circulation*. 2011;124:1001-1011.)

**Key Words:** cardiomyopathy ■ electrophysiology ■ genetics ■ ion channels

Voltage-gated sodium channels play a critical role in the generation and propagation of the cardiac action potential, and mutations in *SCN5A*, the gene encoding the major pore-forming sodium channel  $\alpha$  subunit in the heart (Nav1.5), cause multiple inherited cardiac arrhythmia syndromes, including long-QT syndrome, the Brugada syndrome, isolated cardiac conduction disease, sinus node dysfunction, and atrial fibrillation.<sup>1-7</sup> More recently, *SCN5A* mutations have been associated with dilated cardiomyopathy (DCM), and such DCM mutations have been associated with a similar range of arrhythmias.<sup>8-15</sup>

**Editorial see p 993**  
**Clinical Perspective on p 1011**

The D1275N *SCN5A* mutation was initially reported in a Dutch family affected by atrial standstill, mild conduction

disease, and atrial enlargement but no ventricular structural abnormality; only subjects who carried a variant in the connexin 40 promoter displayed the clinical phenotype.<sup>16</sup> Subsequently, D1275N was implicated in a large family affected by DCM and various arrhythmias such as sinus node dysfunction, atrial and ventricular tachyarrhythmias, and conduction disease.<sup>8,9,17</sup> Most recently, the mutation was reported in a family with atrial tachyarrhythmias, conduction disease, and ventricular enlargement without impaired contractility.<sup>18</sup>

Heterologous expression systems are conventionally used to assess function of ion channel mutations.<sup>2,19</sup> Most studies (including our own data described below) that have compared wild-type and D1275N channels in heterologous expression systems have not shown major differences in the biophysical

Received August 31, 2010; accepted June 9, 2011.

From the Departments of Medicine and Pharmacology (H.W., T.Y., D.M.S., J.S.L., T.C.A., D.W.W., B.L., L.H., S.K., N.K., B.C.K., A.L.G., D.M.R.) and Molecular Physiology and Biophysics (S.B.H., M.A.M.), Vanderbilt University School of Medicine, Nashville, TN; Division of Cardiology, Niigata University Graduate School of Medical and Dental Sciences, Niigata, Japan (H.W.); Division of Cardiology, University of Toronto, Canada (L.H.); Department of Medicine, The First Affiliated Hospital of Nanjing Medical University, Nanjing, China (D.W.W.); and Department of Health and Nutrition, University of Niigata Prefecture, Niigata, Japan (N.T.).

Guest editor for this article was Barry London, MD, PhD.

Correspondence to Dan M. Roden, MD, Director, Oates Institute for Experimental Therapeutics, Assistant Vice-Chancellor for Personalized Medicine, Vanderbilt University School of Medicine, 2215B Garland Ave, 1285 MRBIV Light Hall, Nashville, TN 37232-0575. E-mail dan.roden@vanderbilt.edu  
© 2011 American Heart Association, Inc.

*Circulation* is available at <http://circ.ahajournals.org>

DOI: 10.1161/CIRCULATIONAHA.110.987248

properties of the variant channel.<sup>16,20</sup> Thus, although the mutation has been reported as a cause of unusual phenotypes in a number of kindreds, its relationship to the clinical phenotypes remains uncertain.

To address this discrepancy, we have used recombinase-mediated cassette exchange<sup>21</sup> to engineer mice expressing the mutant human channel (here called DN); we compared the functional properties of these animals with those expressing wild-type human alleles (H) that we previously generated in an identical fashion.<sup>21</sup> The data demonstrate that D1275N causes a severe defect in sodium channel function in vivo, consistent with the reported clinical phenotypes.

## Methods

### Study Subjects

The proband and family members were screened for mutations in *SCN5A* by polymerase chain reaction amplification of coding regions and flanking intronic sequences, followed by direct sequencing of amplicons on an ABI PRISM 3730 DNA Sequence Detection System (Applied Biosystems, Foster City, CA). Informed consent was obtained for presentation of the kindred.

### Animal Model

All studies using animals were approved by the institutional animal care and use committees at Vanderbilt University and performed in accordance with National Institutes of Health guidelines. We have previously modified the *Scn5a* locus in mouse embryonic stem cells to enable the technique of recombinase mediated cassette exchange.<sup>21–23</sup> In our initial studies, we inserted the full-length human *SCN5A* cDNA into the targeted locus.<sup>21</sup> Mice homozygous for the exchanged allele (called H/H) expressed only the human allele and had normal ECGs and ventricular sodium current, supporting the hypothesis that expression of the exchanged allele was under control of endogenous *Scn5a* regulatory mechanisms.

For the present study, we used the same technique to generate DN mice in which the exchanged construct was identical to that previously used for the H/H mice with the exception of a c.3823G→A mutation resulting in p.D1275N and insertion of an FLAG epitope between residues 153 and 154 of the extracellular linker S1–S2 in domain I; the FLAG insertion into S1–S2 linker has previously been found to have no effect on channel gating or cell surface expression.<sup>24,25</sup> We also generated FG mice bearing the wild-type *SCN5A* allele with the FLAG tag. Initial matings between mice heterozygous for engineered alleles resulted in H/H, DN/H, and FG/H mice, and these mice were then bred into the 129/Sv background. H/H, DN/H, and DN/DN mice were generated from DN/H×DN/H matings, and H/H littermates were used as controls for all experiments. To genotype mice, genomic DNA was isolated from mouse tails, and the target *SCN5A* polymerase chain reaction amplicon (c.3688 to c.4082) was incubated with Taq1 (New England Biolabs, Ipswich, MA) and then electrophoresed in agarose gels. Taq1 digests the fragment containing p.D1275 but does not digest that with p.N1275.

### Surface Electrocardiogram

Electrocardiograms were recorded during administration of isoflurane vapor titrated to maintain light anesthesia.<sup>26</sup> Baseline ECG (leads I and II) was recorded for 15 minutes. Heart rate was measured as the average during a 30-second interval at baseline when a steady state was reached during anesthesia. For measurement of all other ECG parameters, 30 seconds of data in each lead were signal averaged with a custom-built LabVIEW program (National Instruments, Austin, TX), and the resultant waveform was analyzed with an electric caliper by an electrophysiologist blind to the genotype.<sup>27</sup> The larger value from each lead was used. QRS duration was measured from the first deflection of the Q wave (or R wave when the Q wave was absent) and the end of the S wave defined as

the point of minimum voltage in the terminal phase of the QRS complex. The QT interval was measured from the beginning of the QRS complex to the end of the T wave defined as the point where the T wave merges with the isoelectric line. Heart rate–corrected QT interval (QTc) was calculated from a formula developed for mice:  $QTc = QT / (RR/100)^{1/2}$ .<sup>28</sup>

### Echocardiogram

Transthoracic echocardiograms were performed on resting conscious mice and analyzed by a sonographer blinded to the genotype. Signals were acquired with a 15-MHz transducer (Sonos 5500 system, Agilent, Santa Clara, CA) at the Murine Cardiovascular Core at Vanderbilt University as previously described.<sup>29</sup>

### Histology

Hearts were fixed overnight in 10% formalin, paraffin embedded, sectioned at 5  $\mu$ m, and stained with Masson trichrome.

### mRNA Quantification

Real-time polymerase chain reaction was conducted with a 7900HT Real-Time Instrument (Applied Biosystems). mRNA was isolated from the left ventricles, and cDNA was synthesized from 2  $\mu$ g of the RNA by use of the Transcriptor First Strand cDNA Synthesis Kit with random hexamer primers (Roche Applied Science, Indianapolis, IL) and used as a template. To generate a standard curve for absolute quantification, genes of interest were subcloned into the pGEM-T vector (Clontech, Mountain View, CA). cDNA and 5 different dilutions of the vector with target DNA were prepared with pre-designed 6-carboxyfluorescein–labeled fluorogenic TaqMan probe and primers (Applied Biosystems) for *SCN5A* (Hs00165693 m1) or  $\beta$ -actin (Mm00607939 S1) in triplicate in the same 96-well plate for real-time polymerase chain reaction amplification. Data were collected with instrument spectral compensation and analyzed by use of absolute quantification and a standard curve with SDS 2.2 software (Applied Biosystems). Each value was normalized to that for  $\beta$ -actin.

### Western Blotting

Protein was extracted from flash-frozen hearts that were pulverized into powder and homogenized in a Dounce apparatus with 1× radioimmunoprecipitation assay buffer. Lysates were centrifuged at 10 000g for 5 minutes, and protein content was analyzed with a bicinchoninic acid assay (Pierce Biochemicals, Rockford, IL). Protein (40 to 100  $\mu$ g) from each cardiac sample was separated by running the sample on a NuPage 8% Tris-acetate gel (Invitrogen, Carlsbad, CA). The protein was transferred to 0.2  $\mu$ m nitrocellulose membranes (Amersham Biosciences, Sweden), which were blocked overnight in 0.05% Tween-20 Tris-buffered saline (TTBS) plus 5% nonfat dry milk at 4°C and then incubated with antibodies targeting anti-Nav1.5 (polyclonal antibody, 1:200; Alomone Labs, Israel) or anti-calnexin (polyclonal antibody, 1:1000; Stressgen Bioreagents, Belgium) at room temperature for 2 hours. Membranes were washed 3 times with TTBS for 10 minutes each and incubated with secondary anti-mouse and anti-rabbit horseradish peroxidase-linked antibodies (Amersham Biosciences) in TTBS at room temperature for 1 hour. The blots were then washed 4 times for 10 minutes each in TTBS. We visualized antibody interactions with the ECL system (Amersham Biosciences).

### Immunostaining/Confocal Microscopy

Unfixed hearts were frozen in Tissue Tek and sectioned at 6  $\mu$ m. Sections were washed in 1× Dulbecco phosphate-buffered saline and then incubated in 1× Dulbecco phosphate-buffered saline containing 0.3% fish gelatin and 0.1% Triton (block) for 1 hour at 4°C. Sections were immunostained with antibodies targeting anti-Nav1.5 (polyclonal antibody 1:50, Alomone Labs) diluted in block solution overnight. Samples were then washed 3 times and incubated with Alexa 488–conjugated goat anti-mouse IgG (1:400, Invitrogen) secondary antibody for 1 hour at room temperature. Then sections

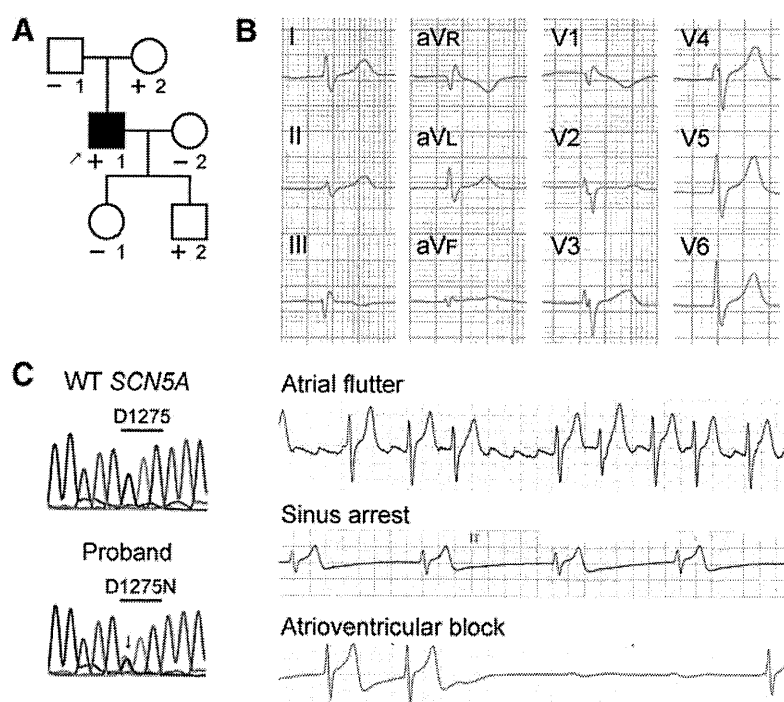


**Figure 1.** D1275N *SCN5A* mutation in a patient with sinus node dysfunction, atrial flutter, and conduction disease. **A**, Pedigree. The proband is indicated by the arrow. Individuals carrying the mutation are indicated (+). Individuals who tested negative for the mutation are indicated (-). Filled symbols indicate phenotype positive. **B**, Electrocardiogram and rhythm strips in the proband. **C**, Heterozygous single-nucleotide change in *SCN5A* (c.3823G→A) resulting in p.D1275N.

were washed and coverslips were applied with Vectashield (Vector Labs, Burlingame, CA). Images were collected with a Zeiss LSM510 Meta confocal imaging system with 20×1.3 NA lens (pinhole equals 1 airy disk) with 2× zoom and analyzed with LSM 4.0 software.

### Sodium Current Recordings

Sodium current was recorded with the whole-cell voltage-clamp technique in single ventricular myocytes isolated by a modified collagenase/protease method or in Chinese hamster ovary (CHO) cells transiently expressing wild-type or D1275N *SCN5A*.<sup>21,30,31</sup> The *SCN5A* DNA (NM 198056) was subcloned into the pBK-CMV vector (Stratagene, La Jolla, CA), and the mutation was prepared with the QuickChange II XL site-directed mutagenesis kit (Stratagene), followed by verification by resequencing. *SCN5A* DNA (1 μg) was transfected with the plasmid encoding the enhanced green fluorescent protein (pEGFP-IRES, Clontech) by use of Fugene6 (Roche Applied Science, Indianapolis, IN) in CHO cells. Cells were grown for 48 hours after transfection before study. Similar methods were used to study the biophysical properties of wild-type and D1275N sodium channels transfected with the sodium channel β1 subunit in human embryonic kidney cells (tsA201). Late sodium current was measured at the end of 200-ms test pulses to -20 mV from a holding potential of -120 mV (interpulse duration, 5 seconds).

The extracellular bath solution contained (in mmol/L) 145 NaCl, 4.0 KCl, 1.0 MgCl<sub>2</sub>, 1.8 CaCl<sub>2</sub>, 10 glucose, and 10 HEPES, pH 7.4 (NaOH), for sodium current recording in CHO and tsA201 cells. Patch pipettes (≈1.5 mol/LΩ) contained (in mmol/L) 10 NaF, 110 CsF, 20 CsCl, 10 EGTA, and 10 HEPES, pH 7.4 (CsOH). To allow recording of sodium current in cardiomyocytes, the external Na<sup>+</sup> concentration was lowered to 5 mmol/L, electrodes with tip resistance <1 mol/LΩ were used, and experiments were conducted at 18°C. Data acquisition was carried out with an Axopatch 200B patch-clamp amplifier and pCLAMP software (version 9.2, Molecular Devices, Sunnyvale, CA). Currents were filtered at 5 kHz and digitized with an analog-to-digital interface (Digidata 1322A, Molecular Devices). To minimize capacitive transients, capacitance and series resistance were adjusted to 70% to 85%. Details of the pulse protocols are presented schematically in the figures.

### Action Potential Recordings

Action potentials from isolated mouse ventricular myocytes were elicited with injection of brief stimulus current (1 to 2 nA, 2 to 6 ms) at 5 Hz in current clamp mode (Axopatch 200A amplifier, Molecular Devices). The extracellular bath solution contained (in mmol/L) NaCl 140, KCl 5.4, CaCl<sub>2</sub> 1.8, MgCl<sub>2</sub> 1, HEPES 5, and glucose 10, pH 7.4 (adjusted by NaOH). Patch pipettes contained (in mmol/L) KCl 110, K<sub>2</sub>-ATP 5, MgCl<sub>2</sub> 1, BAPTA 0.1, and HEPES 10, pH 7.2 (adjusted by KOH). Microelectrodes of 3 to 5 mol/LΩ were used. Data acquisition was carried out with an Axopatch 200B patch-clamp amplifier and pCLAMP. The action potential durations at 50% and 90% repolarization and the action potential amplitude were measured.

### Data Analysis

Results are presented as mean±SEM. The unpaired *t* test was used for comparisons of electrophysiological characteristics between D1275N and wild-type channels expressed in heterologous expression systems. We used ANOVA followed by a post hoc analysis with Bonferroni correction for all of comparisons among the genotypes of mice, except for the linear mixed-effects models with Bonferroni correction for comparisons of in vitro electrophysiological characteristics of mice. All statistical analyses were performed with SPSS, version 12.0 (SPSS Inc, Chicago, IL). A 2-tailed value of *P*<0.05 was considered statistically significant.

## Results

### Clinical Case Presentation

A 19-year-old white man (II-1) presented with recurrent exertional syncope (Figure 1A, arrow). Physical examination and echocardiography were normal, and his ECG demonstrated unusually slow atrial flutter that was conducted 1:1 to the ventricles with hypotension during exertion (Figure 1B). After catheter ablation of the cavo-tricuspid isthmus for atrial flutter, he had atrial standstill, prolonged QRS duration, sinus node dysfunction, high-degree atrioventricular block, and normal QT interval. A cardioverter-defibrillator was implanted. He has been

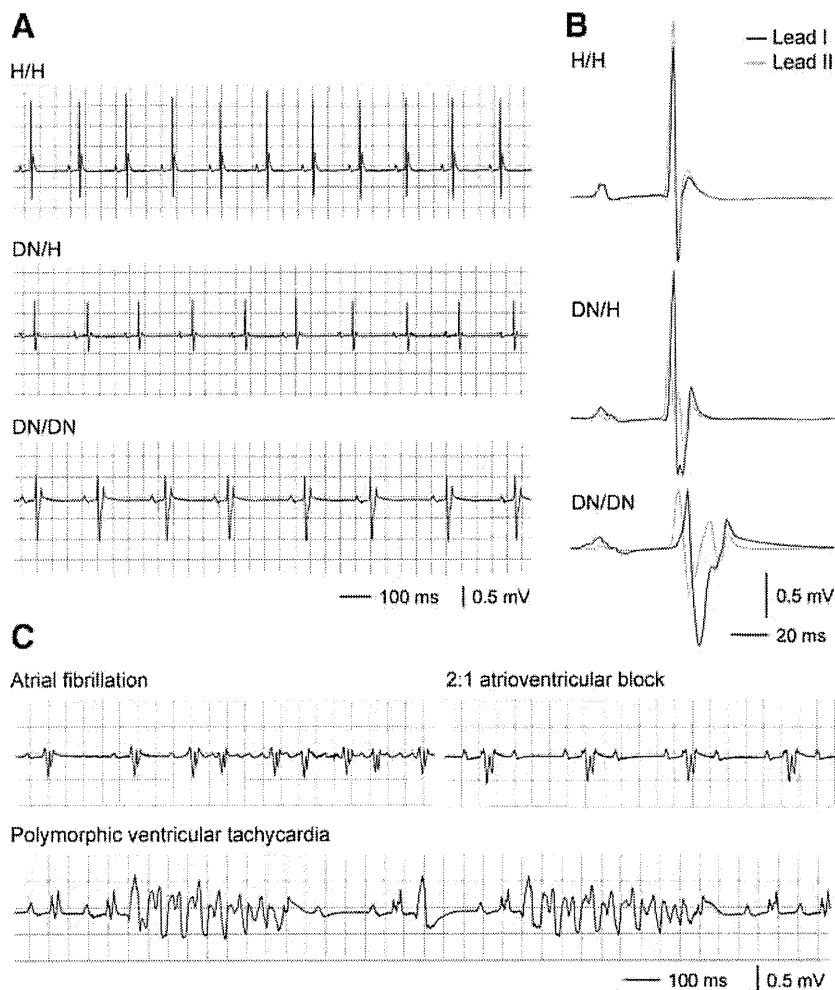


**Figure 2.** Electrocardiography in mice. **A**, Representative ECG traces in lead I at 3 weeks. **B**, Representative signal-averaged ECG traces in leads I (black) and II (gray) at 3 weeks. See Table 1 for detailed results. **C**, Arrhythmias recorded in DN/DN mice at 12 weeks.

asymptomatic for 10 years, and his echocardiography has been normal. We identified a missense mutation in *SCN5A*, c.3823G→A in exon 21 (Figure 1C), resulting in p.D1275N within a transmembrane domain of the protein (segment 3, domain III); the variant connexin 40 associated with atrial standstill in the reported Dutch kindred was absent.<sup>16</sup> Both his mother (I-2) and 1 son (III-2) share the mutation but have no clinical findings.

### DN Mice Are Viable and Display Gene-Dose-Dependent Conduction Slowing and Arrhythmias

The distribution of pups from DN/H×DN/H matings was in Hardy-Weinberg equilibrium (52 H/H, 107 DN/H, 54 DN/DN). During a follow-up of 12 weeks, 1 DN/DN mouse died suddenly, but no DN/H or H/H mice died. ECG recordings revealed that the DN allele caused abnormal phenotypes in a gene-dose-dependent fashion at 3 weeks (Figure 2A and 2B, and Table 1). The DN allele was associated with slow heart rate and slow cardiac conduction (prolongation of the P-wave duration, PR interval, and QRS duration) at 3 weeks, and similar changes were observed at 12 weeks. In mice with ECGs recorded at both 3 and 12 weeks, the prolongation of the P-wave duration, PR interval, and QRS duration associated with the DN

allele was progressive with age. In addition, spontaneous monomorphic and polymorphic ventricular tachycardia was observed in 7 of 9 DN/DN mice during 15-minute recording periods under light anesthesia at 12 weeks, but no arrhythmia was observed in 18 DN/H or 10 H/H littermates studied under the same conditions (Figure 2C). Sinus node dysfunction (n=3), atrioventricular block (second degree or higher; n=4), and atrial fibrillation/tachycardia (n=5) also occurred only in DN/DN mice, not in DN/H or H/H littermates.

### Reduced Contractile Function in DN Mice

There was consistent and statistically significant end-diastolic and end-systolic left ventricular dilatation and calculated left ventricular fractional shortening reduction in a gene-dose-dependent fashion (Figure 3A and Table 2). Histological examination of mouse hearts revealed that the DN allele was associated with ventricular dilatation but was not associated with significant fibrosis or myocyte disarray (Figure 3B). One possibility is that the FLAG tag incorporated into the DN allele contributes to the phenotypes in the DN animals. However, we found no difference in ECG and echocardiographic phenotypes between H/H and FG/FG animals, indicating that the FLAG tag does not



**Table 1. ECG Phenotype**

	H/H	DN/H	DN/DN
At 3 weeks			
n	11	20	9
Heart rate, bpm	388±8	354±8*	335±15*
P-wave duration, ms	13.0±0.6	17.0±0.3*	19.4±0.5*†
PR interval, ms	33.7±0.7	35.6±0.7	44.1±0.9*†
QRS duration, ms	9.8±0.2	11.8±0.3*	22.3±2.2*†
QT interval, ms	48.5±1.9	50.2±1.1	67.6±4.2*†
QTc interval, ms	38.9±1.6	38.5±0.8	50.2±2.5*†
At 12 weeks			
n	10	18	9
Heart rate, bpm	387±8	368±11	317±18*
P-wave duration, ms	14±0.5	18.6±0.3*	27.1±1.2*†
PR interval, ms	37.8±0.8	39.7±0.7	57.1±3.1*†
QRS duration, ms	10.7±0.4	12.9±0.3	33.4±2.7*†
QT interval, ms	51.2±0.6	54.8±0.8	77.9±3.7*†
QTc interval, ms	41.1±0.6	42.8±0.9	55.9±1.8*†
Ratio of week 12 to week 3, %‡			
n	9	14	6
Heart rate, bpm	101±2	103±4	119±18
P-wave duration, ms	104±4	112±5	143±11*†
PR interval, ms	113±3	115±2	125±5*
QRS duration, ms	111±4	116±4	154±14*†
QT interval, ms	106±5	114±3	117±11
QTc interval, ms	106±5	115±3	123±6

QTc=QT/(RR/100)<sup>1/2</sup> (mouse-specific).

\**P*<0.05 vs H/H; †*P*<0.05 vs DN/H.

‡For animals with measurements at both time points.

contribute to the ventricular dysfunction or other phenotypes observed in DN animals.

### Sodium Current Is Reduced in DN Myocytes

The manifest conduction slowing in DN mice is consistent with loss of sodium channel function. However, sodium current amplitudes and gating observed with heterologous expression of wild-type and D1275N channels in CHO cells were nearly indistinguishable (Figure 4A through 4C and Table 3). In CHO cells, there was also no difference in the voltage dependence of activation and inactivation or in the time course of inactivation. Similarly, only minor differences were observed between wild-type and D1275N channels coexpressed with  $\beta$ 1 subunits in tsA201 cells; current amplitudes were nearly identical, but there were a slight shift in the voltage dependence of activation and an increase in late sodium current (percent to peak current: wild-type, 0.22±0.05%, n=7; D1275N, 1.34±0.11%, n=8; *P*<0.001; Figure 4D through 4F and Table 3).

In contrast, in ventricular cardiomyocytes, peak sodium current amplitude was markedly reduced in DN/H and DN/DN mice compared with H/H littermates (Figure 5A and 5B and Table 3). In addition, late sodium current was increased in DN/DN mice compared with DN/H and H/H littermates (Figure 5C). We also found that sodium current in

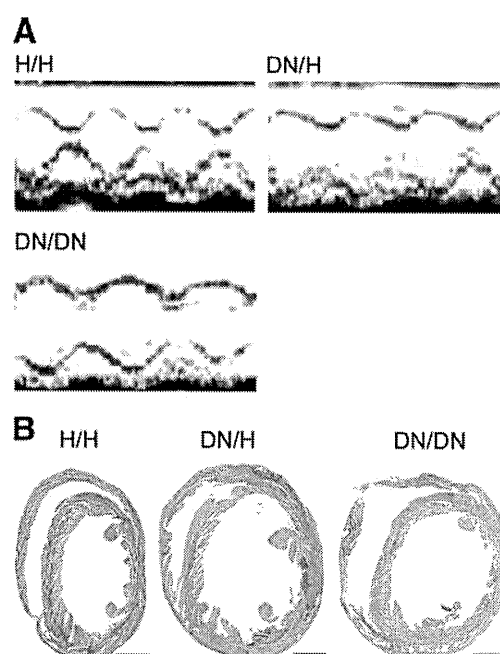


**Figure 3.** Dilated cardiomyopathy phenotype. **A**, Representative echocardiograms showing prominent increased end-systolic dimensions in DN/H and DN/DN mice at 12 weeks. See Table 2 for summary results. **B**, Masson trichrome staining in mice hearts. Scale bars indicate 1 mm.

DN/DN myocytes displayed consistent changes in gating. The voltage dependence of inactivation was positively shifted in DN/DN mice compared with DN/H and H/H mice (Figure 5D). The time course of inactivation was slower in DN/DN mice compared with DN/H and H/H littermates (time constant at -30 mV: DN/DN, 5.5±0.2 milliseconds; DN/H, 2.8±0.1 milliseconds; H/H, 2.7±0.2 milliseconds; Figure 5E and 5F). There was no difference in the voltage dependence of activation. The DN allele was associated with decreased action potential amplitude, consistent with the decrease in peak sodium current, and with prolonged action potential duration, consistent with the increase in late current (Figure 6).

### Sodium Channel Protein Abundance Is Reduced in DN Myocytes

Western blotting showed a reduction in sodium channel protein abundance associated with the DN allele, and the changes were much more dramatic in DN/DN compared with DN/H hearts (Figure 7A and 7B). The abundance of

**Table 2. Echocardiographic Phenotype at 12 Weeks**

	H/H (n=9)	DN/H (n=19)	DN/DN (n=12)
Septal wall, mm	0.75±0.02	0.72±0.02	0.69±0.03
Posterior wall, mm	0.51±0.03	0.47±0.01	0.51±0.04
Left ventricle, mm			
End diastole	3.01±0.08	3.09±0.08	3.33±0.07*
End systole	1.49±0.09	1.76±0.05*	2.01±0.05*†
Fractional shortening, %	52.0±1.6	43.1±0.7*	39.9±0.7*†

\**P*<0.05 vs H/H; †*P*<0.05 vs DN/H.

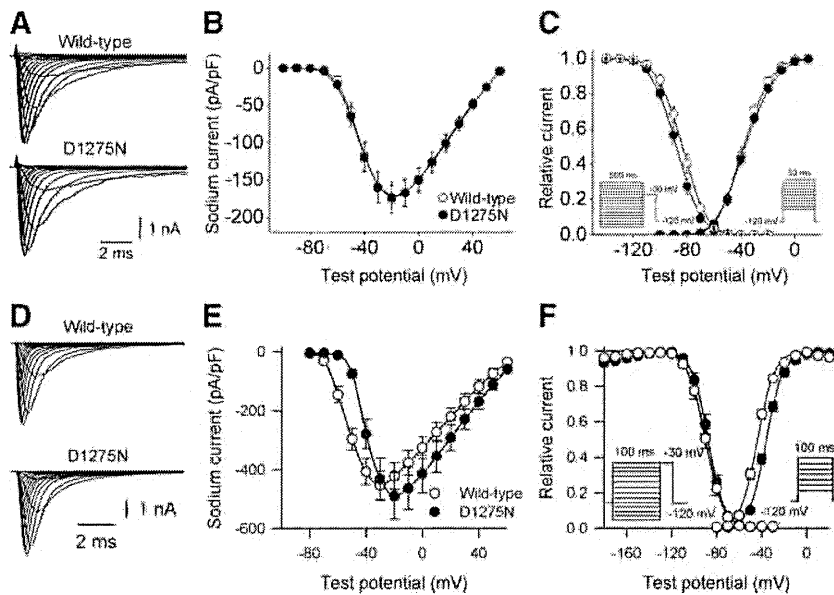


**Figure 4.** Wild-type and D1275N sodium current in Chinese hamster ovary cells (A through C) and tsA201 cells (D through F). Wild-type or D1275N channels were coexpressed with  $\beta 1$  subunits in tsA201 cells. A and D, Representative current traces. See Table 3 for summary results. B and E, Current voltage relationships. C and F, Voltage dependence of activation and inactivation. The pulse protocols are shown in the inset.

the control calnexin protein was similar among H/H (reference,  $100 \pm 6\%$ ), DN/H ( $103 \pm 4\%$  of H/H), and DN/DN mice ( $100 \pm 5\%$  of H/H) ( $P = NS$  for each). Although sodium current and sodium channel protein were reduced in DN/DN and DN/H mice compared with H/H littermates, real-time polymerase chain reaction showed that *SCN5A* transcript levels were elevated in mice with the DN allele (Figure 7C). Expression levels of  $\beta$ -actin transcripts were similar among H/H (reference,  $100 \pm 1\%$ ), DN/H ( $100 \pm 1\%$  of H/H), and DN/DN mice ( $102 \pm 5\%$  of H/H) ( $P = NS$  for each). Immunostaining experiments were conducted in heart sections at 3 weeks (Figure 8). The DN allele was associated with reduced levels of cell surface expression. Notably, staining was obvious on the lateral myocyte aspects in H/H hearts but was nearly absent in DN/DN hearts stained under identical conditions.

### Discussion

The D1275N mutation has been associated with sinus node dysfunction, conduction abnormalities, tachyarrhythmias, and contractile dysfunction.<sup>8,9,16–18</sup> However, in previous studies, the evidence implicating D1275N as the causative mutation has been weak: for example, in the large Dutch kindred, the contribution of an additional connexin variant was invoked to explain why only a minority of subjects displayed a clinical phenotype, but that variant was absent in the proband reported here. In addition, D1275N does not generate major changes in sodium channel function in heterologous expression studies.<sup>8,9,16–18</sup> Thus, despite the previous and the present clinical case reports, the formal possibility remained that D1275N does not actually contribute to the abnormal phenotypes. To address the role of this (and other) variants in mediating sodium channel-

**Table 3. Sodium Channel Gating in Heterologous Expression Systems and Ventricular Cardiomyocytes**

	Peak Current Density at $-30$ mV		Voltage Dependence of Activation		Voltage Dependence of Inactivation	
	pA/pF	n	$V_{1/2}$ , mV	n	$V_{1/2}$ , mV	n
CHO cells						
Wild type	$-160 \pm 20$	25	$-35.4 \pm 0.6$	25	$-84.5 \pm 1.0$	24
D1275N	$-159 \pm 21$	28	$-34.7 \pm 0.6$	28	$-88.4 \pm 0.8$	27
tsA201 cells						
Wild type	$-454 \pm 48$	16	$-47.7 \pm 1.1$	16	$-89.4 \pm 0.7$	19
D1275N	$-432 \pm 71$	13	$-35.7 \pm 1.1 \dagger$	13	$-88.0 \pm 1.6$	18
Cardiomyocytes*						
H/H	$-40.9 \pm 2.9$	10	$-44.1 \pm 1.0$	10	$-84.1 \pm 1.0$	10
DN/H	$-19.2 \pm 3.1 \ddagger$	12	$-44.3 \pm 1.4$	12	$-81.2 \pm 1.1$	12
DN/DN	$-9.3 \pm 1.1 \S \parallel$	12	$-45.6 \pm 0.9$	12	$-76.5 \pm 0.8 \S \parallel$	12

CHO indicates Chinese hamster ovary; n, number of cells. Study conditions differ for heterologous expression systems and cardiomyocytes as described in Methods.

\*Cardiomyocytes from 3 mice for each genotype.

$\dagger P < 0.001$  versus wild type;  $\ddagger P < 0.05$  versus H/H;  $\S P < 0.01$  versus H/H;  $\parallel P < 0.01$  vs DN/H.

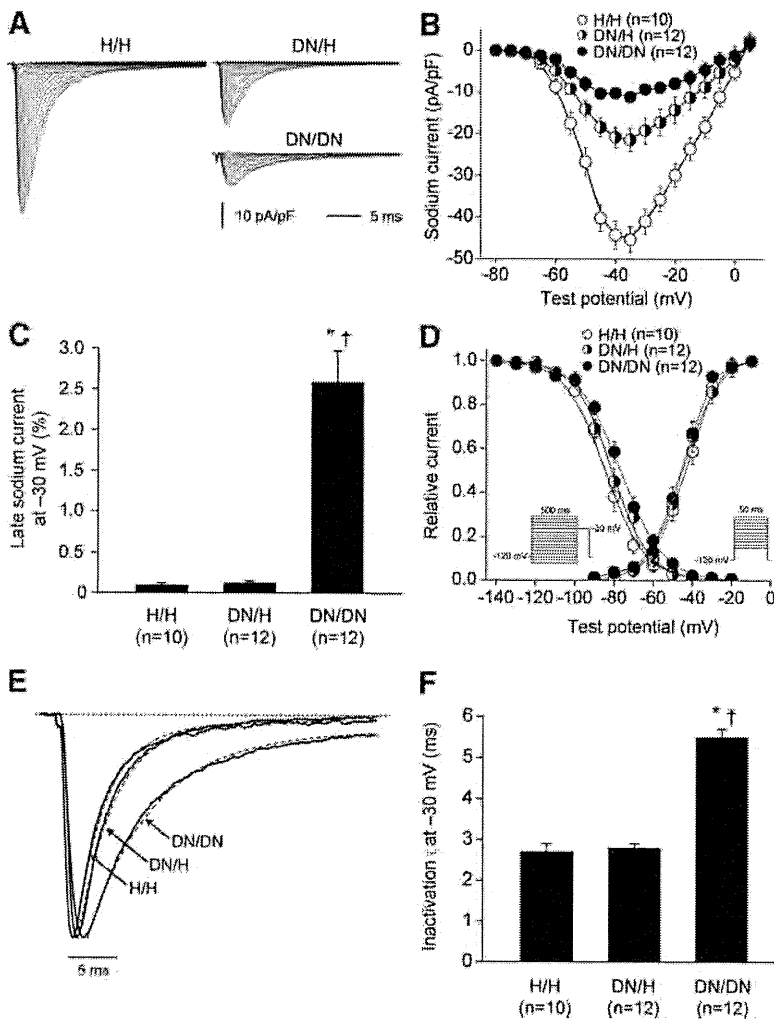


**Figure 5.** Sodium current in male ventricular cardiomyocytes at 3 weeks showing altered sodium channel function by the DN allele. **A**, Representative current traces in H/H, DN/H, and DN/DN cells. See Table 3 for summary results. **B**, Current voltage relationships. **C**, Late sodium current at  $-30$  mV. Late current amplitude was normalized to peak current amplitude. **D**, Voltage dependence of activation and inactivation. **E** and **F**, Inactivation time constant ( $\tau$ ) at  $-30$  mV. \* $P < 0.001$  vs H/H; † $P < 0.001$  vs DN/H. n indicates the number of cardiomyocytes from 3 mice.

linked clinical phenotypes, we generated a series of mouse lines in which the murine cardiac sodium channel was ablated and human alleles were substituted in the murine *Scn5a* locus. The technique of recombinase-mediated cassette exchange allowed us to place wild-type or mutant human sodium channel cDNAs in the murine cardiac sodium channel locus.<sup>21</sup> We have previously reported that this approach eliminates expression of the murine channel and that sodium currents from unmodified wild-type murine ventricular myocytes and those expressing wild-type human *SCN5A* are indistinguishable, indicating that expression of the exchanged sequence is determined by endogenous sodium channel regulatory mechanisms.<sup>21</sup>

### DN Mice Display Sodium Channel Dysfunction

Sodium current amplitude was similar between D1275N and wild-type channels when expressed in heterologous expression systems in the present study in either the absence or presence of  $\beta 1$  subunit.<sup>16</sup> This is in agreement with most results previously reported, although 1 group has found that D1275N channels generate significantly less current than wild-type channels in tsA201 cells; the reason for this discrepancy is unknown.<sup>20</sup> In our mouse model, D1275N was associated with decreased levels of sodium

channel protein by Western analysis of total ventricular protein, decreased expression of sodium channels at the ventricular myocyte surface, and marked reduction of sodium current. In addition, we observed increased late current and altered voltage-dependence of channel inactivation. Thus, channel dysfunction conferred by D1275N becomes evident in the myocyte environment. The major change, reduction in peak sodium current, could represent decreased cell surface expression and/or altered gating of the channel protein. One possible explanation in either case is altered interactions with sodium channel partners, present in myocytes and absent in CHO and tsA201 cells.<sup>32,33</sup> There is precedent for such a hypothesis; the E1053K *SCN5A* mutation, which is associated with a loss of sodium channel function phenotype, has no effect on current density when studied in heterologous expression systems but abolishes binding of the channel to ankyrin-G and reduces cell surface expression and sodium current in cultured cardiomyocytes.<sup>34</sup> However, although E1053K affects channel gating under heterologous expression,<sup>34</sup> altered channel gating by D1275N was found only in the mice, not in heterologous systems, in our study. This is clearly not a general rule because channel dysfunction observed with heterologous expression of other mutants

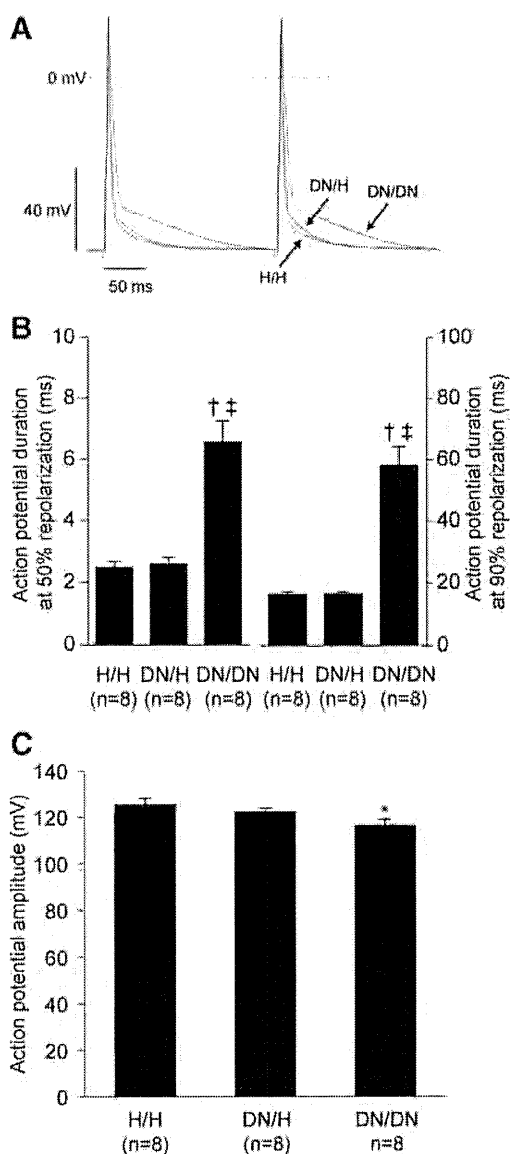


**Figure 6.** Action potential in male ventricular cardiomyocytes at 3 weeks. **A**, Representative action potential traces. **B**, Action potential duration at 50% and 90% repolarization. **C**, Action potential amplitude. \* $P < 0.05$  vs H/H; † $P < 0.01$  vs H/H; ‡ $P < 0.01$  vs DN/H. n Indicates the number of cardiomyocytes from 3 mice.

(delKQP1505–1507 and 1795insD) recapitulates phenotypes observed clinically and in genetically modified mice.<sup>7,35–37</sup>

### Association of Sodium Channel Mutations With Cardiomyopathy

In addition to arrhythmias, *SCN5A* mutations have been associated with cardiomyopathy.<sup>8–15</sup> To date, 12 rare variants in *SCN5A* have been identified in cardiomyopathy, and all of the variants have been associated with arrhythmia phenotypes that result from loss of sodium channel function.<sup>8–15</sup> In our mouse model, the loss of sodium channel function by D1275N is consistent with biophysical properties of other *SCN5A* mutations associ-

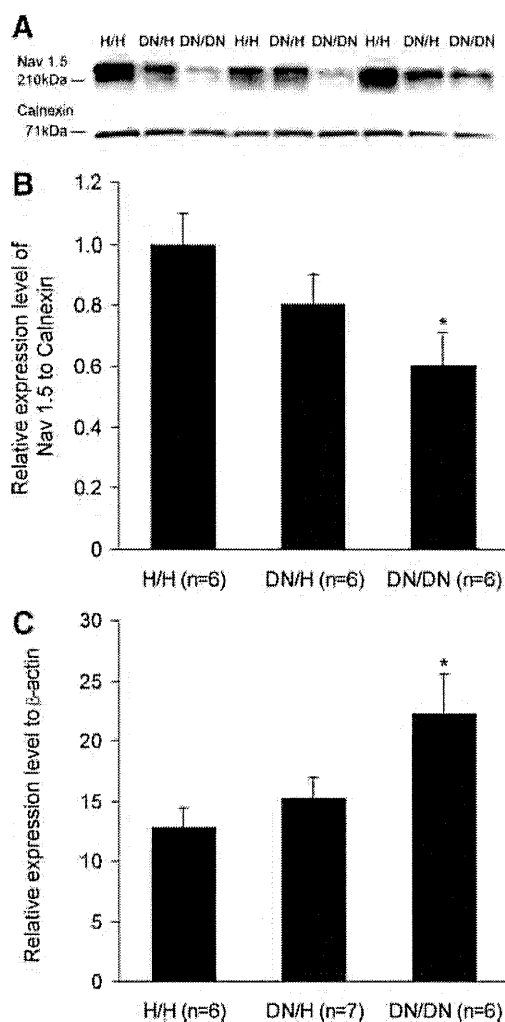


**Figure 7.** Sodium channel expression levels at 3 weeks. **A**, Representative Western blots in ventricles. **B**, Sodium channel expression levels normalized to those of H/H. Calnexin was used as the loading control. **C**, Relative expression levels of *SCN5A* transcript normalized to those of  $\beta$ -actin in ventricle. \* $P < 0.05$  vs H/H.

ated with DCM,<sup>10,11,38</sup> and findings in clinical and experimental studies suggest that a marked reduction in sodium current is critical for the development of cardiomyopathy.<sup>13,14,39,40</sup> In prior studies, mice with 90% reduction of *Scn5a* expression level developed cardiac dysfunction,<sup>39</sup> whereas heterozygous *Scn5a* knockdown mice (*Scn5a*<sup>+/-</sup>) display normal cardiac function.<sup>40</sup> In our study, mice expressing D1275N, one of the initially reported *SCN5A* mutations in a cardiomyopathy kindred,<sup>8,9</sup> showed a reduction in sodium current with disrupted channel gating and developed evident cardiomyopathy at 12 weeks. This is consistent with other reports describing that both R814Q occurring homozygously and the compound heterozygous occurrence of the W156X and R225W are associated with cardiomyopathy.<sup>13,14</sup> In these settings, the cardiomyopathy phenotype is generally absent in heterozygotes.<sup>13,14</sup>

Among 12 rare variants in *SCN5A* associated with cardiomyopathy, 7 are located in transmembrane domains, and 6 of them, including D1275N, are predicted to change

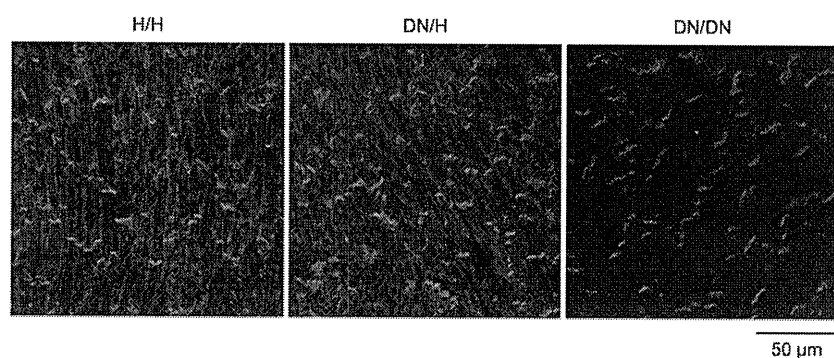


**Figure 8.** Immunostaining for sodium channel (Nav1.5) at 3 weeks. Heart sections from the ventricles were stained with anti-Nav1.5 (green). Note the obvious lateral staining in the H/H heart and its absence in the DN/DN heart.

the electric charge of substituted amino acids.<sup>8–15</sup> These substitutions may lead to changes in channel structure, resulting in altered channel gating and/or reduced channel expression levels directly or by disrupted interaction with sodium channel accessory proteins.

Although this study and previous work strongly imply that loss of sodium channel function has a critical role for development of cardiomyopathy,<sup>10,41</sup> the mechanisms remain controversial. The surface ECG tracings in DN mice (Figure 2) not only demonstrate gene-dose-dependent conduction slowing but also suggest altered activation sequence (with ECG complex splintering); thus, electromechanical dyssynchrony, a well-recognized cause of cardiac contractile dysfunction,<sup>42</sup> may be sufficient to explain the DCM phenotype. Another possibility raised by a recent report that suggests 2 pools of sodium channel protein in heart is that the mutant channel does not target the appropriate subcellular domain to support normal cell propagation.<sup>43</sup> Among causative genes for DCM, cytoskeletal components such as syntrophins and dystrophins have been associated with *SCN5A* channel, and disrupted interaction with such proteins may result in cardiomyopathy.<sup>44–46</sup> Although *SCN5A* mutations have been associated with cardiac fibrosis,<sup>3,40,47</sup> we did not observe fibrosis when the mice carrying the DN allele developed cardiac dysfunction. It has been reported that *SCN5A*-related DCM phenotype usually develops later (>10 years) than the onset of arrhythmia phenotypes, suggesting a possibility that the DCM phenotype is secondarily mediated by arrhythmia.<sup>8–10,48</sup> In our study, however, the cardiomyopathy phenotype was evident relatively early, in the absence of sustained arrhythmia. Taking these results together, we propose that sodium channel dysfunction and electromechanical dyssynchrony represent the primary pathophysiology for DCM in this setting.

### Conclusions

We found that the D1275N *SCN5A* mutation was associated with cardiomyopathy and multiple arrhythmias in vivo, in line with clinical findings in our and other studies.<sup>8,9,16–18</sup> Although D1275N did not generate serious channel dysfunction when studied in heterologous expression systems, the mutation produced extensive channel dysfunction, notably marked reduction in peak current amplitude, and a cardiomyopathy phenotype in our mouse model. Further experiments along the lines outlined above

are required to elucidate the precise mechanisms for channel dysfunction and how this leads to the DCM phenotype. Defining the mechanisms underlying the disconnect between the results in heterologous expression systems and those in myocytes will contribute to furthering our understanding of the variable phenotypes and penetrance of D1275N and other *SCN5A* mutations.

### Acknowledgments

We thank Christiana Ingram, Justine Stassun, Laura Short, and Wei Zhang at Vanderbilt University for their assistance in performing or analyzing this work. We also acknowledge the expert performance of the staff of the Vanderbilt Transgenic Mouse/Embryonic Stem Cell Shared Resource for the blastocyst microinjections. Imaging of histological and immunohistochemistry samples was performed at the VUMC Cell Imaging Shared Resource.

### Sources of Funding

This work was supported by grants from the US Public Health Service, Bethesda, MD (HL65962, HL49989, DK42502, and DK72473) and from the Fondation Leducq, Paris, France (Trans-Atlantic Network of Excellence: Preventing Sudden Cardiac Death, 05-CVD-01). The Murine Cardiovascular Core is supported in part by U24 DK59637, Cardiovascular Core, Mouse Metabolic Physiology Centers, Vanderbilt University. The VUMC Cell Imaging Shared Resource is supported by NIH grants CA68485, DK20593, DK58404, HD15052, DK59637, and EY08126.

### Disclosures

None.

### References

- Wang Q, Shen J, Splawski I, Atkinson D, Li Z, Robinson JL, Moss AJ, Towbin JA, Keating MT. *SCN5A* mutations associated with an inherited cardiac arrhythmia, long QT syndrome. *Cell*. 1995;80:805–811.
- Chen Q, Kirsch GE, Zhang D, Brugada R, Brugada J, Brugada P, Potenza D, Moya A, Borggrefe M, Breithardt G, Ortiz-Lopez R, Wang Z, Antzelevitch C, O'Brien RE, Schulze-Bahr E, Keating MT, Towbin JA, Wang Q. Genetic basis and molecular mechanism for idiopathic ventricular fibrillation. *Nature*. 1998;392:293–296.
- Schott JJ, Alshinawi C, Kyndt F, Probst V, Hoorntje TM, Hulsbeek M, Wilde AA, Escande D, Mannens MM, Le Marec H. Cardiac conduction defects associate with mutations in *SCN5A*. *Nat Genet*. 1999; 23:20–21.
- Benson DW, Wang DW, Dymnt M, Knilans TK, Fish FA, Strieper MJ, Rhodes TH, George AL Jr. Congenital sick sinus syndrome caused by recessive mutations in the cardiac sodium channel gene (*SCN5A*). *J Clin Invest*. 2003;112:1019–1028.
- Ellinor PT, Nam EG, Shea MA, Milan DJ, Ruskin JN, MacRae CA. Cardiac sodium channel mutation in atrial fibrillation. *Heart Rhythm*. 2008;5:99–105.
- Darbar D, Kannankeril PJ, Donahue BS, Kucera G, Stubblefield T, Haines JL, George AL Jr, Roden DM. Cardiac sodium channel (*SCN5A*)

- variants associated with atrial fibrillation. *Circulation*. 2008;117:1927–1935.
7. Bezzina C, Veldkamp MW, van Den Berg MP, Postma AV, Rook MB, Viersma JW, van Langen IM, Tan-Sindhunata G, Bink-Boelkens MT, van Der Hout AH, Mannens MM, Wilde AA. A single Na<sup>+</sup> channel mutation causing both long-QT and Brugada syndromes. *Circ Res*. 1999;85:1206–1213.
  8. McNair WP, Ku L, Taylor MR, Fain PR, Dao D, Wolfel E, Mestroni L. *SCN5A* mutation associated with dilated cardiomyopathy, conduction disorder, and arrhythmia. *Circulation*. 2004;110:2163–2167.
  9. Olson TM, Michels VV, Ballew JD, Reyna SP, Karst ML, Herron KJ, Horton SC, Rodeheffer RJ, Anderson JL. Sodium channel mutations and susceptibility to heart failure and atrial fibrillation. *JAMA*. 2005;293:447–454.
  10. Ge J, Sun A, Pajajani V, Wang S, Su C, Yang Z, Li Y, Wang S, Jia J, Wang K, Zou Y, Gao L, Wang K, Fan Z. Molecular and clinical characterization of a novel *SCN5A* mutation associated with atrioventricular block and dilated cardiomyopathy. *Circ Arrhythmia Electrophysiol*. 2008;1:83–92.
  11. Shi R, Zhang Y, Yang C, Huang C, Zhou X, Qiang H, Grace AA, Huang CL, Ma A. The cardiac sodium channel mutation delQKP 1507–1509 is associated with the expanding phenotypic spectrum of LQT3, conduction disorder, dilated cardiomyopathy, and high incidence of youth sudden death. *Europace*. 2008;10:1329–1335.
  12. Kapplinger JD, Tester DJ, Alders M, Benito B, Berthet M, Brugada J, Brugada P, Fressart V, Guerschicoff A, Harris-Kerr C, Kamakura S, Kyndt F, Koopmann TT, Miyamoto Y, Pfeiffer R, Pollevick GD, Probst V, Zumhagen S, Vatta M, Towbin JA, Shimizu W, Schulze-Bahr E, Antzelevitch C, Salisbury BA, Guicheney P, Wilde AA, Brugada R, Schott JJ, Ackerman MJ. An international compendium of mutations in the *SCN5A*-encoded cardiac sodium channel in patients referred for Brugada syndrome genetic testing. *Heart Rhythm*. 2010;7:33–46.
  13. Bezzina CR, Rook MB, Groenewegen WA, Herfst LJ, van der Wal AC, Lam J, Jongsma HJ, Wilde AA, Mannens MM. Compound heterozygosity for mutations (W156X and R225W) in *SCN5A* associated with severe cardiac conduction disturbances and degenerative changes in the conduction system. *Circ Res*. 2003;92:159–168.
  14. Frigo G, Rampazzo A, Bauce B, Pilichou K, Boffagna G, Danieli GA, Nava A, Martini B. Homozygous *SCN5A* mutation in Brugada syndrome with monomorphic ventricular tachycardia and structural heart abnormalities. *Europace*. 2007;9:391–397.
  15. Chen S, Chung MK, Martin D, Rozich R, Tchou PJ, Wang Q. SNP S1103Y in the cardiac sodium channel gene *SCN5A* is associated with cardiac arrhythmias and sudden death in a white family. *J Med Genet*. 2002;39:913–915.
  16. Groenewegen WA, Firouzi M, Bezzina CR, Vliex S, van Langen IM, Sandkuijl L, Smits JP, Hulsbeek M, Rook MB, Jongsma HJ, Wilde AA. A cardiac sodium channel mutation cosegregates with a rare connexin40 genotype in familial atrial standstill. *Circ Res*. 2003;92:14–22.
  17. Greenlee PR, Anderson JL, Lutz JR, Lindsay AE, Hagan AD. Familial automaticity-conduction disorder with associated cardiomyopathy. *West J Med*. 1986;144:33–41.
  18. Laitinen-Forsblom PJ, Makynen P, Makynen H, Yli-Mayry S, Virtanen V, Kontula K, Aalto-Setälä K. *SCN5A* mutation associated with cardiac conduction defect and atrial arrhythmias. *J Cardiovasc Electrophysiol*. 2006;17:480–485.
  19. Bennett PB, Yazawa K, Makita N, George AL Jr. Molecular mechanism for an inherited cardiac arrhythmia. *Nature*. 1995;376:683–685.
  20. Gui J, Wang T, Jones RP, Trump D, Zimmer T, Lei M. Multiple loss-of-function mechanisms contribute to *SCN5A*-related familial sick sinus syndrome. *PLoS One*. 2010;5:e10985.
  21. Liu K, Hipkens S, Yang T, Abraham R, Zhang W, Chopra N, Knollmann B, Magnuson MA, Roden DM. Recombinase-mediated cassette exchange to rapidly and efficiently generate mice with human cardiac sodium channels. *Genesis*. 2006;44:556–564.
  22. Jones JR, Shelton KD, Magnuson MA. Strategies for the use of site-specific recombinases in genome engineering. *Methods Mol Med*. 2005;103:245–257.
  23. Lauth M, Spreafico F, Dethleffsen K, Meyer M. Stable and efficient cassette exchange under non-selectable conditions by combined use of two site-specific recombinases. *Nucleic Acids Res*. 2002;30:e115.
  24. Ye B, Valdivia CR, Ackerman MJ, Makielski JC. A common human *SCN5A* polymorphism modifies expression of an arrhythmia causing mutation. *Physiol Genomics*. 2003;12:187–193.
  25. Liu K, Yang T, Viswanathan PC, Roden DM. New mechanism contributing to drug-induced arrhythmia: rescue of a misprocessed LQT3 mutant. *Circulation*. 2005;112:3239–3246.
  26. Knollmann BC, Chopra N, Hlaing T, Akin B, Yang T, Etensohn K, Knollmann BE, Horton KD, Weissman NJ, Holinstat I, Zhang W, Roden DM, Jones LR, Franzini-Armstrong C, Pfeifer K. *Casq2* deletion causes sarcoplasmic reticulum volume increase, premature Ca<sup>2+</sup> release, and catecholaminergic polymorphic ventricular tachycardia. *J Clin Invest*. 2006;116:2510–2520.
  27. Casimiro MC, Knollmann BC, Ebert SN, Vary JC Jr, Greene AE, Franz MR, Grinberg A, Huang SP, Pfeifer K. Targeted disruption of the *Kcnq1* gene produces a mouse model of Jervell and Lange-Nielsen Syndrome. *Proc Natl Acad Sci USA*. 2001;98:2526–2531.
  28. Mitchell GF, Jeron A, Koren G. Measurement of heart rate and Q-T interval in the conscious mouse. *Am J Physiol*. 1998;274(pt 2):H747–H751.
  29. Rottman JN, Ni G, Brown M. Echocardiographic evaluation of ventricular function in mice. *Echocardiography*. 2007;24:83–89.
  30. Knollmann BC, Knollmann-Ritschel BE, Weissman NJ, Jones LR, Morad M. Remodelling of ionic currents in hypertrophied and failing hearts of transgenic mice overexpressing calsequestrin. *J Physiol*. 2000;525(pt 2):483–498.
  31. Watanabe H, Koopmann TT, Le Scouarnec S, Yang T, Ingram CR, Schott JJ, Demolombe S, Probst V, Anselme F, Escande D, Wiesfeld AC, Pfeufer A, Kaab S, Wichmann HE, Hasdemir C, Aizawa Y, Wilde AA, Roden DM, Bezzina CR. Sodium channel beta1 subunit mutations associated with Brugada syndrome and cardiac conduction disease in humans. *J Clin Invest*. 2008;118:2260–2268.
  32. Abriel H. Roles and regulation of the cardiac sodium channel Na(v)1.5: Recent insights from experimental studies. *Cardiovasc Res*. 2007;76:381–389.
  33. Meadows LS, Isom LL. Sodium channels as macromolecular complexes: implications for inherited arrhythmia syndromes. *Cardiovasc Res*. 2005;67:448–458.
  34. Mohler PJ, Rivolta I, Napolitano C, LeMaillet G, Lambert S, Priori SG, Bennett V. Nav1.5 E1053K mutation causing Brugada syndrome blocks binding to ankyrin-G and expression of Nav1.5 on the surface of cardiomyocytes. *Proc Natl Acad Sci USA*. 2004;101:17533–17538.
  35. Dumaine R, Wang Q, Keating MT, Hartmann HA, Schwartz PJ, Brown AM, Kirsch GE. Multiple mechanisms of Na<sup>+</sup> channel-linked long-QT syndrome. *Circ Res*. 1996;78:916–924.
  36. Nuyens D, Stengl M, Dugarmaa S, Rossenbacker T, Compennolle V, Rudy Y, Smits JF, Flameng W, Clancy CE, Moons L, Vos MA, Deweerchin M, Benndorf K, Collen D, Carmeliet E, Carmeliet P. Abrupt rate accelerations or premature beats cause life-threatening arrhythmias in mice with long-QT3 syndrome. *Nat Med*. 2001;7:1021–1027.
  37. Remme CA, Verkerk AO, Nuyens D, van Ginneken AC, van Brunschot S, Belterman CN, Wilders R, van Roon MA, Tan HL, Wilde AA, Carmeliet P, de Bakker JM, Veldkamp MW, Bezzina CR. Overlap syndrome of cardiac sodium channel disease in mice carrying the equivalent mutation of human *SCN5A*-1795insD. *Circulation*. 2006;114:2584–2594.
  38. Keller DI, Acharfi S, Delacretaz E, Benammar N, Rotter M, Pfammatter JP, Fressart V, Guicheney P, Chahine M. A novel mutation in *SCN5A*, delQKP 1507–1509, causing long QT syndrome: role of Q1507 residue in sodium channel inactivation. *J Mol Cell Cardiol*. 2003;35:1513–1521.
  39. Hesse M, Kondo CS, Clark RB, Su L, Allen FL, Geary-Joo CT, Kunnathu S, Severson DL, Nygren A, Giles WR, Cross JC. Dilated cardiomyopathy is associated with reduced expression of the cardiac sodium channel *Scn5a*. *Cardiovasc Res*. 2007;75:498–509.
  40. Royer A, van Veen TA, Le Bouter S, Marionneau C, Griol-Charhibi V, Leoni AL, Steenman M, van Rijen HV, Demolombe S, Goddard CA, Richer C, Escoubet B, Jarry-Guichard T, Colledge WH, Gros D, de Bakker JM, Grace AA, Escande D, Charpentier F. Mouse model of *SCN5A*-linked hereditary Lenegre's disease: age-related conduction slowing and myocardial fibrosis. *Circulation*. 2005;111:1738–1746.
  41. Nguyen TP, Wang DW, Rhodes TH, George AL Jr. Divergent biophysical defects caused by mutant sodium channels in dilated cardiomyopathy with arrhythmia. *Circ Res*. 2008;102:364–371.
  42. Cazeau S, Leclercq C, Lavergne T, Walker S, Varma C, Linde C, Garrigue S, Kappenberger L, Haywood GA, Santini M, Baillet C, Daubert JC. Effects of multisite biventricular pacing in patients with heart failure and intraventricular conduction delay. *N Engl J Med*. 2001;344:873–880.

43. Petitprez S, Zmoos AF, Ogrodnik J, Balse E, Raad N, El-Haou S, Albesa M, Bittihn P, Luther S, Lehnart SE, Hatem SN, Coulombe A, Abriel H. SAP97 and dystrophin macromolecular complexes determine two pools of cardiac sodium channels Nav1.5 in cardiomyocytes. *Circ Res*. 2011;108:294–304.
44. Towbin JA, Bowles NE. The failing heart. *Nature*. 2002;415:227–233.
45. Karkkainen S, Peuhkurinen K. Genetics of dilated cardiomyopathy. *Ann Med*. 2007;39:91–107.
46. Gavillet B, Rougier JS, Domenighetti AA, Behar R, Boixel C, Ruchat P, Lehr HA, Pedrazzini T, Abriel H. Cardiac sodium channel Nav1.5 is regulated by a multiprotein complex composed of syntrophins and dystrophin. *Circ Res*. 2006;99:407–414.
47. Coronel R, Casini S, Koopmann TT, Wilms-Schopman FJ, Verkerk AO, de Groot JR, Bhuiyan Z, Bezzina CR, Veldkamp MW, Linnenbank AC, van der Wal AC, Tan HL, Brugada P, Wilde AA, de Bakker JM. Right ventricular fibrosis and conduction delay in a patient with clinical signs of Brugada syndrome: a combined electrophysiological, genetic, histopathologic, and computational study. *Circulation*. 2005;112:2769–2777.
48. Shinbane JS, Wood MA, Jensen DN, Ellenbogen KA, Fitzpatrick AP, Scheinman MM. Tachycardia-induced cardiomyopathy: a review of animal models and clinical studies. *J Am Coll Cardiol*. 1997;29:709–715.

### CLINICAL PERSPECTIVE

A conventional approach to characterize the function of ion channel mutations is to compare wild-type and variant channel function by heterologous expression in mammalian, noncardiac cells like Chinese hamster ovary or human embryonic kidney cells. The cardiac sodium channel mutation D1275N has been reported in multiple individuals and families with a range of phenotypes, including arrhythmias and dilated cardiomyopathy; however, conventional heterologous expression studies have not identified major differences between wild-type and D1275N function. Thus, it has even been uncertain whether this mutation causes the clinical phenotypes with which it has been associated. In this study, we addressed this issue by studying mice in which the cardiac sodium channel locus had been disrupted and replaced with full-length human wild-type or D1275N mutant sodium channels. We observed slowed and disordered cardiac conduction and decreased contractile function in mice bearing the mutation; mice with 2 D1275N alleles displayed worse phenotypes than those with 1 variant allele. In vitro electrophysiological studies identified reduced peak cardiac sodium current as a key defect, and this is consistent with the observed reduced conduction velocity. The major clinical implication of these findings is that heterologous expression may be insufficient to assess mutant channel function. In addition, the data lend support to the concept that sodium channel mutations are associated not only with arrhythmias but also with dilated cardiomyopathy phenotypes. The mutant mice will be an invaluable tool to dissect mechanisms underlying these findings.

# Electrocardiographic Characteristics and *SCN5A* Mutations in Idiopathic Ventricular Fibrillation Associated With Early Repolarization

Hiroshi Watanabe, MD, PhD, FESC; Akihiko Nogami, MD, PhD; Kimie Ohkubo, MD, PhD; Hiro Kawata, MD, PhD; Yuka Hayashi, MD; Taisuke Ishikawa, DVM; Takeru Makiyama, MD, PhD; Satomi Nagao, MD; Nobue Yagihara, MD; Naofumi Takehara, MD, PhD; Yuichiro Kawamura, MD, PhD; Akinori Sato, MD, PhD; Kazuki Okamura, MD, PhD; Yukio Hosaka, MD, PhD; Masahito Sato, MD, PhD; Satoki Fukae, MD, PhD; Masaomi Chinushi, MD, PhD; Hirotaka Oda, MD, PhD; Masaaki Okabe, MD, PhD; Akinori Kimura, MD, PhD; Koji Maemura, MD, PhD; Ichiro Watanabe, MD, PhD, FHR; Shiro Kamakura, MD, PhD; Minoru Horie, MD, PhD; Yoshifusa Aizawa, MD, PhD; Wataru Shimizu, MD, PhD; Naomasa Makita, MD, PhD

**Background**—Recently, we and others reported that early repolarization (J wave) is associated with idiopathic ventricular fibrillation. However, its clinical and genetic characteristics are unclear.

**Methods and Results**—This study included 50 patients (44 men; age,  $45 \pm 17$  years) with idiopathic ventricular fibrillation associated with early repolarization, and 250 age- and sex-matched healthy controls. All of the patients had experienced arrhythmia events, and 8 (16%) had a family history of sudden death. Ventricular fibrillation was inducible by programmed electric stimulation in 15 of 29 patients (52%). The heart rate was slower and the PR interval and QRS duration were longer in patients with idiopathic ventricular fibrillation than in controls. We identified nonsynonymous variants in *SCN5A* (resulting in A226D, L846R, and R367H) in 3 unrelated patients. These variants occur at residues that are highly conserved across mammals. His-ventricular interval was prolonged in all of the patients carrying an *SCN5A* mutation. Sodium channel blocker challenge resulted in an augmentation of early repolarization or development of ventricular fibrillation in all of 3 patients, but none was diagnosed with Brugada syndrome. In heterologous expression studies, all of the mutant channels failed to generate any currents. Immunostaining revealed a trafficking defect in A226D channels and normal trafficking in R367H and L846R channels.

**Conclusions**—We found reductions in heart rate and cardiac conduction and loss-of-function mutations in *SCN5A* in patients with idiopathic ventricular fibrillation associated with early repolarization. These findings support the hypothesis that decreased sodium current enhances ventricular fibrillation susceptibility. (*Circ Arrhythm Electrophysiol.* 2011;4:874-881.)

**Key Words:** arrhythmia ■ sodium channel ■ electrophysiology ■ genetics ■ mutations

Early repolarization or J-wave is characterized by an elevation at the junction between the end of the QRS

## Clinical Perspective on p 881

complex and the beginning of the ST-segment (J-point) in a 12-lead ECG and generally has been considered benign for

decades.<sup>1</sup> However, early repolarization can be observed under various negative biological conditions, such as low body temperature and ischemia,<sup>2-4</sup> and there is increasing evidence that early repolarization is associated with an increased risk of ventricular fibrillation and sudden cardiac death.<sup>5-7</sup>

Received February 2, 2011; accepted October 5, 2011.

From the Division of Cardiology (H.W., Y.H., S.N., N.Y., A.S., K.O., M.C., Y.A.), Niigata University School of Medicine, Niigata; Division of Heart Rhythm Management (A.N.), Yokohama Rosai Hospital, Yokohama; Division of Cardiology (K.O., I.W.), Department of Medicine, Nihon University School of Medicine, Tokyo; Division of Arrhythmia and Electrophysiology (H.K., S.K., W.S.), Department of Cardiovascular Medicine, National Cerebral and Cardiovascular Center, Suita; Department of Molecular Pathogenesis (T.I., A.K.), Medical Research Institute, Tokyo Medical and Dental University, Tokyo; Department of Cardiovascular Medicine (T.M.), Kyoto University Graduate School of Medicine, Kyoto; Department of Internal Medicine (N.T., Y.K.), Division of Cardiovascular Respiratory and Neurology, Asahikawa Medical University, Asahikawa; Department of Cardiology (Y.H., H.O.), Niigata City General Hospital, Niigata; Cardiovascular Center (M.S., M.O.), Tachikawa General Hospital, Nagaoka; Departments of Cardiovascular Medicine (S.F., K.M.) and Molecular Physiology (N.M.), Nagasaki University Graduate School of Biomedical Sciences, Nagasaki; Department of Cardiovascular and Respiratory Medicine (M.H.), Shiga University of Medical Science, Shiga, Japan.

Correspondence to Hiroshi Watanabe, MD, PhD, FESC, Division of Cardiology, Niigata University Graduate School of Medical and Dental Sciences, 1-754 Asahimachidori, Niigata 951-8510 Japan. E-mail [hiroshi7@med.niigata-u.ac.jp](mailto:hiroshi7@med.niigata-u.ac.jp)

© 2011 American Heart Association, Inc.

*Circ Arrhythm Electrophysiol* is available at <http://circep.ahajournals.org>

DOI: 10.1161/CIRCEP.111.963983



In previous studies, including our own, early repolarization in the inferior or lateral leads was associated with pathogenesis in idiopathic ventricular fibrillation.<sup>5,6</sup> Moreover, early repolarization in the right precordial leads also has been associated with idiopathic ventricular fibrillation.<sup>8</sup> Heritability of early repolarization has been shown in a recent population-based study,<sup>9</sup> and as in other arrhythmia syndromes such as long QT syndrome and Brugada syndrome,<sup>10</sup> ion channel genes are responsible for idiopathic ventricular fibrillation associated with early repolarization.<sup>11–13</sup> A mutation in *KCNJ8*, which encodes a pore-forming subunit of the ATP-sensitive potassium channel, has been identified in idiopathic ventricular fibrillation with early repolarization.<sup>11,14</sup> Mutations in L-type calcium channel genes, including *CACNA1C*, *CACNB2B*, and *CACNA2D1*, also have been associated with idiopathic ventricular fibrillation with early repolarization.<sup>12</sup>

In this study, we compared electrocardiographic parameters between patients with idiopathic ventricular fibrillation and healthy controls and found that heart rate and cardiac conduction were slow in patients with idiopathic ventricular fibrillation. Furthermore, we screened patients with idiopathic ventricular fibrillation for mutations in *SCN5A*, which encodes the predominant cardiac sodium channel  $\alpha$  subunit and is critical for cardiac conduction. Here, we present the clinical and in vitro electrophysiological characteristics in idiopathic ventricular fibrillation associated with early repolarization.

## Methods

### Study Populations

This study included patients with idiopathic ventricular fibrillation and early repolarization who were referred to our institutions. Patients were diagnosed with idiopathic ventricular fibrillation if they had no structural heart disease as identified using echocardiography, coronary angiography, and left ventriculography. Baseline electrophysiological studies without antiarrhythmic drugs were performed based on the indication of each institution. Early repolarization was defined as an elevation of the J-point, either as QRS slurring or notching  $\geq 0.1$  mV  $\geq 2$  consecutive leads in the 12-lead ECG.<sup>5</sup> Patients were excluded if they had a short QT interval (corrected QT interval using Bazett formula  $< 340$  ms) or a long QT interval (corrected QT interval  $> 440$  ms) in the 12-lead ECG.<sup>15,16</sup> All patients received sodium channel blocker challenge, and patients with Brugada type ST-segment elevations at baseline or after sodium channel blocker challenge were excluded.<sup>17</sup> Twelve-lead electrocardiograms recorded in the absence of antiarrhythmic drugs were compared between patients with idiopathic ventricular fibrillation and control subjects who were matched to patients with idiopathic ventricular fibrillation based on gender and age (patient: control ratio, 1:5). Control subjects were selected from 86 068 consecutive electrocardiograms stored in the ECG database in Niigata University Medical and Dental Hospital from May 7, 2003 to July 2, 2009.<sup>18</sup> Control subjects who had a normal QT interval (corrected QT interval, 360 to 440 ms) and no cardiovascular disease or medication use were included. Control subjects with Brugada type ST-segment elevations or early repolarization were excluded.

### Genetic Analysis

All probands and family members who participated in the study gave written informed consent before genetic and clinical investigations in accordance with the standards of the Declaration of Helsinki and local ethics committees. Genetic analysis was performed on genomic

DNA extracted from peripheral white blood cells using standard methods. The coding regions of *KCNQ1*, *KCNH2*, *SCN5A*, *KCNE1*, *KCNE2*, and *KCNJ8* were amplified by PCR using exon-flanking intronic primers,<sup>19–21</sup> and direct DNA sequencing was performed using ABI 310, 3130, and 3730 genetic analyzers (Applied Biosystems, Foster City, CA).<sup>22</sup>

### Generation of Expression Vectors and Transfection in Mammalian Cell Lines

Full-length human *SCN5A* cDNA was subcloned into the mammalian expression plasmid pcDNA3.1+ (Invitrogen, Carlsbad, CA).<sup>22</sup> Mutant constructs were prepared using a QuikChange site-directed mutagenesis kit (Stratagene, La Jolla, CA) according to the manufacturer's instructions. The human cell line tsA201 was transiently transfected with wild-type or mutant *SCN5A* plasmid using Lipofectamine LTX (Invitrogen), in combination with a bicistronic plasmid (pCD8-IRES-h $\beta$ 1) encoding CD8 and the human sodium channel  $\beta$ 1 subunit (h $\beta$ 1) to visually identify cells expressing heterologous h $\beta$ 1 using Dynabeads M-450 CD8 (Invitrogen).<sup>22</sup> Electrophysiological measurements were performed 24 to 72 hours after transfection.

### Electrophysiology

Sodium currents were recorded using the whole-cell patch clamp technique as previously described.<sup>22</sup> Electrode resistance ranged from 0.8 to 1.5 mol/L $\Omega$ . Data were acquired using an Axopatch 200B patch clamp amplifier and pCLAMP8 software (Axon Instruments). Sodium currents were filtered at 5 kHz ( $-3$  dB, 4-pole Bessel filter) and were digitally sampled at 50 kHz using an analog-to-digital interface (Digidata 1322A; Molecular Devices, Sunnyvale, CA). Experiments were performed at room temperature (20 to 22°C). Voltage errors were minimized using series resistance compensation (generally 80%). Cancellation of the capacitance transients and leak subtraction were performed using an online P/4 protocol. The time from establishing the whole-cell configuration to the onset of recording was consistent (5 minutes) between cells to exclude possible time-dependent shifts of steady-state inactivation. The pulse protocol cycle time was 10 s. The data were analyzed using Clampfit 10 (Molecular Devices) and SigmaPlot 9 software (Aspire Software International, Ashburn, VA). The holding potential was  $-120$  mV. The bath solution contained the following (in mmol/L): 145 NaCl, 4 KCl, 1.8 CaCl<sub>2</sub>, 1 MgCl<sub>2</sub>, 10 HEPES, and 10 glucose, pH 7.35 (adjusted with NaOH). The pipette solution (intracellular solution) contained the following (in mmol/L): 10 NaF, 110 CsF, 20 CsCl, 10 EGTA, and 10 HEPES, pH 7.35 (adjusted with CsOH).

### Immunocytochemistry

For immunocytochemistry, the FLAG epitope was inserted between residues 153 and 154 of the extracellular linker S1-S2 in domain I. The FLAG insertion into the S1-S2 linker previously has been shown to have no effect on channel gating or cell surface expression.<sup>22,23</sup> Immunocytochemistry was performed in HEK293 cells transfected with wild-type or mutant *SCN5A* plasmid as described previously.<sup>22,24</sup> After 48 hours of transfection, the cells were washed with phosphate-buffered saline, fixed in 4% paraformaldehyde, and permeabilized with 0.15% Triton X-100 in phosphate-buffered saline with 3% bovine serum albumin. Then the cells were stained with anti-FLAG polyclonal antibody (F7425; Sigma-Aldrich, St Louis, MO; 1:100) for 1 hour at room temperature. Protein reacting with antibody was visualized with Alexa Fluor 568-labeled secondary antibody (A-11011, Invitrogen, 1:1000). Images were collected using a Zeiss LSM 510 laser confocal microscope and analyzed using LSM 4.0 software.

### Data Analysis

Differences in parameters between patients with idiopathic ventricular fibrillation and control subjects were analyzed using conditional logistic regression models. To exclude the effects of multicollinearity among electrocardiographic parameters, each electrocar-

**Table 1. Electrocardiographic Parameters**

	IVF Patients N=50	Controls N=250	OR (95% CI)/ 10 Unit Increase	P Value
Male sex, N (%)	44 (88)	220 (88)	...	...
Age, y	45±17	45±16	...	...
Heart rate, beats/min	62±9	70±14	0.62 (0.47–0.81)	<0.001
PR interval, ms	175±34	147±20	1.32 (1.22–1.43)	<0.001
QRS interval, ms	96±14	89±8	1.63 (1.31–2.02)	<0.001
QTc, ms	388±25	397±22	0.85 (0.75–0.98)	0.02

IVF indicates idiopathic ventricular fibrillation; OR, odds ratio; QTc, corrected QT interval.

diographic parameter was separately tested in the logistic models. All statistical analyses were performed with SPSS, version 12.0 (SPSS Inc, Chicago, IL). A 2-sided  $P<0.05$  was considered statistically significant. Values are expressed as mean±SD. The study protocol was approved by the ethics committee of each institution.

## Results

We identified 50 patients with idiopathic ventricular fibrillation and early repolarization (44 men [88%]; mean age, 45±17 years). All of the patients had experienced arrhythmia events, and 8 (16%) had a family history of sudden death.

Electrocardiographic parameters were compared between 50 patients with idiopathic ventricular fibrillation and 250 healthy control subjects without cardiovascular disease and not taking medication who were matched with gender and age (Table 1). The heart rate was slower, and the PR interval and QRS duration were longer in patients with idiopathic ventricular fibrillation compared with control subjects. The corrected QT interval was shorter in patients with idiopathic ventricular fibrillation than control subjects. No patient with idiopathic ventricular fibrillation showed type I Brugada electrocardiograms in repeated recordings.<sup>25</sup> Sodium channel blockers were administered in all patients, and Brugada type electrocardiograms were not provoked in any of these patients.<sup>25</sup> Electrophysiological study was performed in 29

patients. His-ventricular interval was 48±9 ms, and 4 patients had prolonged His-ventricular time  $\geq 55$  ms.<sup>26</sup> Ventricular fibrillation was inducible by programmed electric stimulation in 15 patients (52%).

We screened for mutations in *SCN5A* in 26 unrelated patients with idiopathic ventricular fibrillation and identified 3 mutations (A226D, R367H, and L846R) in 3 patients (Figure 1, Table 2). R367H and L846R are predicted to be located in the pore region. These mutations were not found in the genomes of 200 healthy control individuals. Two of the patients exhibited prolongation of the PR interval, and sodium channel blocker challenge was negative for Brugada syndrome in all of them. Alignment of the amino acid sequences from multiple species demonstrated that the amino acids substituted by mutations are highly conserved, supporting the importance of these amino acids. A226D and L846R, but not R367H, are predicted to change the electric charge of substituted amino acids.

A missense mutation, A226D (Figure 1A), was identified in a 36-year-old man (patient 1) resuscitated from ventricular fibrillation. He had experienced multiple episodes of syncope. The physical examination and echocardiography were normal. His ECG showed prolongation of the PR interval and early repolarization in leads II, III, and aVF, and J-point/ST-segment elevation in lead V1 (Figure 2A). Administration of pilsicainide augmented early repolarization in the inferior leads and induced ventricular fibrillation, but did not produce a type I Brugada ECG in the right precordial leads (Figure 2B). Electrophysiological study revealed prolongation of His-ventricular interval (68 ms), and ventricular fibrillation was induced by programmed electric stimulation. The patient's family history was negative for syncope, sudden cardiac death, and epilepsy.

A missense mutation L846R (Figure 1B) was identified in a 27-year-old man (patient 2). He was admitted after multiple episodes of syncope, and polymorphic ventricular tachycardia was documented when he lost consciousness. The physical examination and echocardiography were normal. His ECG

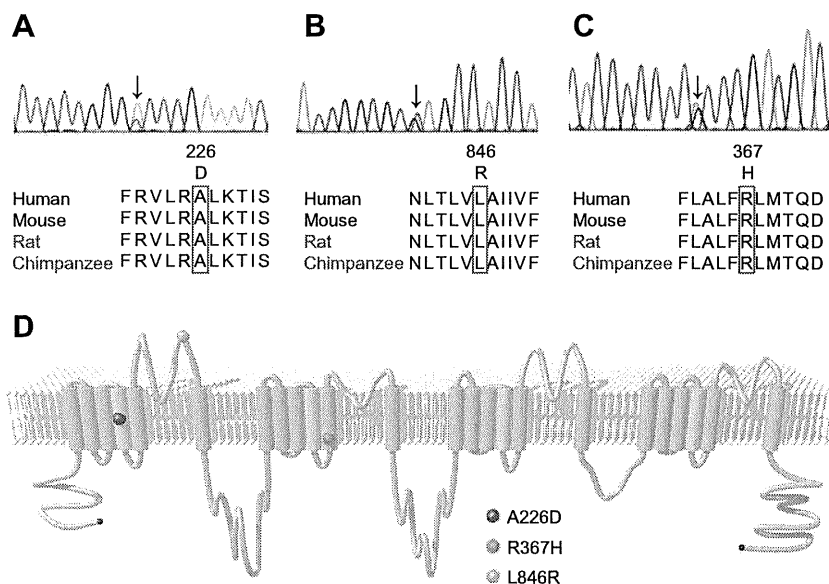


**Figure 1.** Mutations in *SCN5A* identified in patients with idiopathic ventricular fibrillation associated with early repolarization. **A**, The c.677C→A mutation in *SCN5A* resulting in p.A226D found in patient 1. **B**, The c.2537T→G mutation in *SCN5A*, resulting in p.L846R found in patient 2. **C**, The c.1100G→A mutation in *SCN5A*, resulting in p.R367H found in patient 3. We previously reported the R367H mutation (modified from Takehara et al<sup>27</sup>). **D**, Predictive topology of the *SCN5A* channel. Circles indicate the locations of the mutations.

**Table 2. Characteristics of Idiopathic Ventricular Fibrillation Patients With *SCN5A* Mutations**

Patient No.	Sex	Age at Onset (y)	Family History of SCD	Presenting Symptom	Location of J Wave	Other ECG Abnormalities	Response to Sodium Channel Blocker	Amino Acid Substitution
1	M	36	N	Aborted SCD	II, III, aVF, V1	PR prolongation	Augmentation of J-point amplitude and VF	A226D
2	M	27	Y	Aborted SCD	I, II, III, aVF	PR prolongation	Marked QRS prolongation and VF	L846R
3	F	37	N	Aborted SCD	II, III, aVF, V2	N	Augmentation of J-point amplitude and marked QRS prolongation	R367H

ECG indicates electrocardiogram; SCD, sudden cardiac death.

showed prolongation of the PR interval and early repolarization in lead III (Figure 2C). During the recovery phase of exercise testing, the amplitude of the J-point/ST-segment was augmented in leads I, II, III, and aVF, and ventricular fibrillation was induced. Pilsicainide caused marked prolongation of QRS duration and augmented the J-point/ST-segment amplitude in leads V1 and V2, followed by the development of ventricular fibrillation (Figure 2C and 2D). Pilsicainide did not produce a type I Brugada ECG. During electrophysiological study, His-ventricular interval was 55 ms. His uncle died suddenly.

We previously reported a missense mutation R367H in patient 3 as a case with Brugada syndrome (Figure 1C).<sup>27</sup>

However, idiopathic ventricular fibrillation associated with early repolarization was diagnosed at a later time because a type 1 Brugada ECG has never been seen spontaneously or after the administration of sodium channel blocker in more than 1 right precordial lead, and thus the diagnostic criteria for Brugada syndrome were not fulfilled.<sup>25</sup> When the patient admitted to the hospital after recurrent episodes of syncope, early repolarization was present in the inferior and right precordial leads (Figure 2E). After sinus pause, early repolarization was augmented in leads II, III, and aVF, followed by the development of ventricular fibrillation after a few hours of the admission (Figure 2F). Procainamide further exaggerated early repolarization but did not produce a type I

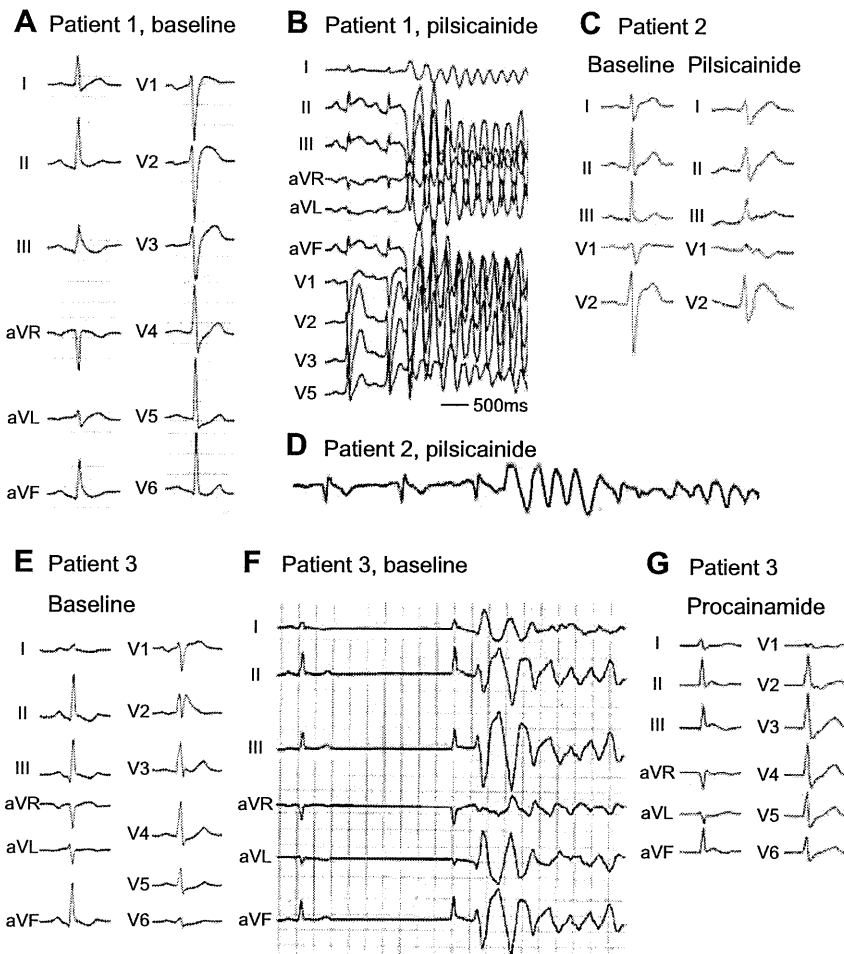


**Figure 2.** Electrocardiograms of patients with idiopathic ventricular fibrillation and a mutation in *SCN5A*. **A**, Early repolarization was present in the inferior and right precordial leads in patient 1. **B**, After administration of pilsicainide, early repolarization was augmented and ventricular fibrillation developed. **C** and **D**, Pilsicainide caused marked prolongation of QRS duration and J-point elevation in the right precordial leads, followed by the development of ventricular fibrillation in patient 2. **E**, Early repolarization was present in the inferior leads and right precordial leads in patient 3. **F**, The augmentation of early repolarization after sinus pause, followed by ventricular fibrillation. **G**, After the administration of procainamide, early repolarization was augmented in the inferior. In all patients, sodium channel blockers did not provoke a type I Brugada ECG. **E**, **F**, and **G** were modified from Takehara et al.<sup>27</sup>

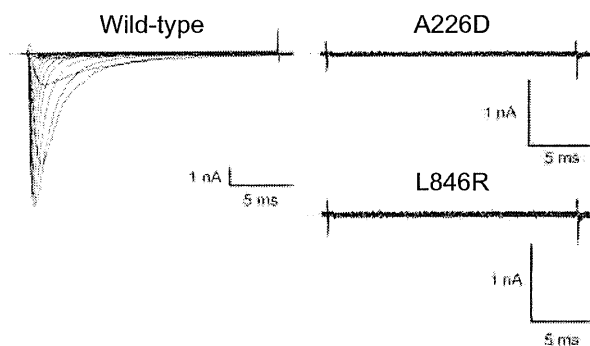


**Figure 3.** Electrophysiological characteristics of the *SCN5A* mutants. Representative traces of sodium current demonstrating that all of the mutant channels failed to generate any currents. We previously reported that R367H mutant fails to generate any currents.<sup>27</sup>

Brugada ECG (Figure 2G). During electrophysiological study, His-ventricular time was prolonged (65 ms) and ventricular fibrillation was not induced. The patient's family history was negative for syncope, sudden cardiac death, and epilepsy.

The electrophysiological characteristics of the mutant sodium channels were assessed in transfected mammalian cells using the whole-cell patch-clamp technique. Figure 3 shows representative current traces in cells expressing wild-type or mutant *SCN5A* channels. There was no detectable current in A226D, R367H,<sup>27</sup> and L846R mutant channels. Immunostaining revealed that cells expressing A226D channels showed cytoplasmic fluorescence, while cells expressing wild-type channels showed marked peripheral fluorescence, suggesting that the mutation results in trafficking defect (Figure 4). Cells expressing R367H channels and those expressing L846R channels showed a similar fluorescence pattern to wild-type channels, suggesting that these mutations do not affect trafficking.

### Discussion

In this study, patients with idiopathic ventricular fibrillation associated with early repolarization exhibited slower heart rate and slower cardiac conduction properties than did controls. We found rare, nonsynonymous variants in *SCN5A* in patients who had idiopathic ventricular fibrillation associated with early repolarization. These variants affect highly conserved residues, and all of the mutant *SCN5A* channels failed to generate any currents when expressed in heterologous expression systems. Immunostaining experiments suggested 2 possible mechanisms for the sodium channel dysfunction by the *SCN5A* mutations, a defect of channel trafficking to cell surface in A226D and critical alterations of the structures required for the sodium ion permeation or gating in R367H and L846R that are predicted to be located at the pore region.

Loss-of-function mutations in *SCN5A* are associated with a wide range of inherited arrhythmia syndromes, including Brugada syndrome, progressive cardiac conduction disease, and sick sinus syndrome.<sup>28–30</sup> Furthermore, our results suggest that *SCN5A* is a causative gene of idiopathic ventricular fibrillation associated with early repolarization. Evidence supporting disease causality of the mutations includes the

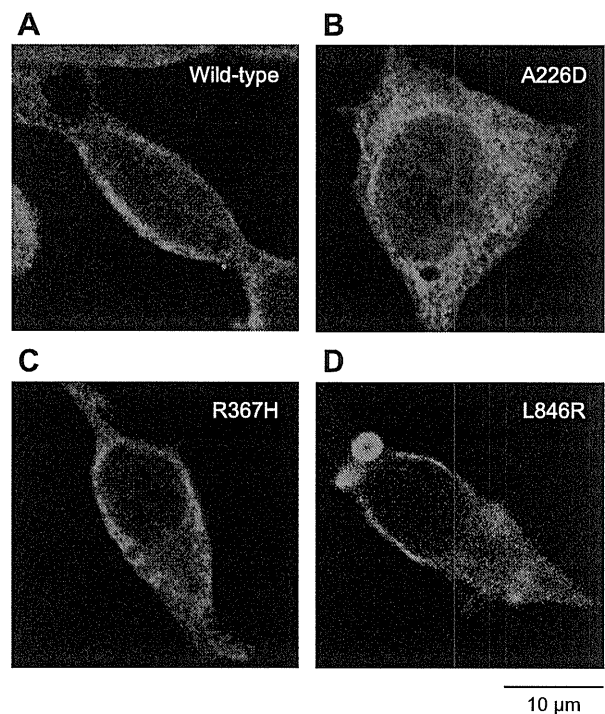


**Figure 4.** Representative confocal microscopy images. **A**, Cells expressing wild-type *SCN5A* channels showed marked peripheral fluorescence. **B**, Cells expressing A226D channels showed cytoplasmic fluorescence. **C** and **D**, Cells expressing R367H channels and those expressing L846R channels showed a similar fluorescence pattern to wild-type channels.

identification of 3 mutations in 3 unrelated probands who shared similar clinical phenotypes and the loss of sodium channel function effects in heterologous expression systems in all of the mutant channels.

Although our findings suggest that loss of sodium channel function plays a role in idiopathic ventricular fibrillation associated with early repolarization, the mechanisms of early repolarization are not understood well. In wedge preparations of canine ventricles, early repolarization results from increased action potential notches at the ventricular epicardium by either a decrease in inward currents or an increase in outward currents.<sup>31</sup> A mutation in *KCNJ8*, which encodes the ATP-sensitive potassium channel, recently has been identified in idiopathic ventricular fibrillation associated with early repolarization.<sup>11</sup> The *KCNJ8* mutation has shown gain-of-function effects in ATP-sensitive potassium channels in heterologous expression studies,<sup>14</sup> and augmentation of ATP-sensitive potassium currents results in the development of ventricular fibrillation in wedge preparations.<sup>32</sup> Decreased calcium currents also have been proposed as a mechanism for idiopathic ventricular fibrillation associated with early repolarization.<sup>33</sup> Mutations in L-type calcium channel genes, including *CACNA1C*, *CACNB2B*, and *CACNA2D1*, recently have been identified; however, functional studies are not yet available.<sup>12</sup> Our findings that mutant *SCN5A* channels displayed loss of sodium channel function, resulting in a decrease of inward currents, are consistent with findings in prior studies and with the proposed mechanism.<sup>11,12,14,33</sup>